

(200)
R290
no. 74-96

SEARCH FOR GEOTHERMAL SEISMIC NOISE
IN THE EAST MESA AREA, IMPERIAL VALLEY, CALIFORNIA

by

H. M. Iyer

United States Geological Survey
345 Middlefield Road
Menlo Park, California 94025

July, 1974

✓
U. S. Geological Survey

OPEN FILE REPORT

Number 74-96

[Reports - Open
file series]

This report is preliminary and has
not been edited or reviewed for
conformity with Geological Survey
standards and nomenclature.

(200)
R290
no. 74-96

(200)
R290
no. 74-96

SEARCH FOR GEOTHERMAL SEISMIC NOISE
IN THE EAST MESA AREA, IMPERIAL VALLEY, CALIFORNIA

by



H. M. Iyer

United States Geological Survey
345 Middlefield Road
Menlo Park, California 94025

July, 1974

U. S. Geological Survey. *Reports—open file series*

OPEN FILE REPORT

Number 74-96

This report is preliminary and has not been edited or reviewed for conformity with Geological Survey standards and nomenclature.

2051579

Table of Contents

	Page
ABSTRACT	1
INTRODUCTION	2
EXPERIMENTAL METHODS	3
NOISE SOURCES IN EAST MESA	6
Freeway Noise	6
East High Line Canal Noise	8
Agricultural Noise	11
All American Canal and Power Drop No. 4 Noise	11
Wind Noise	14
Variation of Regional Noise during the Experiment	14
SPATIAL VARIATION OF NOISE	16
Evaluation of Average Noise Amplitude	17
SPECTRAL STUDIES	34
COHERENCE AND DIRECTION STUDIES	36
Spatial Variation of Coherence	40
Direction Studies	46
CONCLUSIONS	49
ACKNOWLEDGEMENTS	50
REFERENCES	51

SEARCH FOR GEOTHERMAL SEISMIC NOISE IN THE
EAST MESA AREA, IMPERIAL VALLEY, CALIFORNIA

by

H. M. Iyer

ABSTRACT

The U. S. Geological Survey made seismic noise measurements in the East Mesa area of Imperial Valley, California, to find out if a noise anomaly was associated with the Mesa thermal anomaly. Thirty-three locations were occupied in the area using slow-speed tape-recording seismic systems. One of the stations (CEN) was operated close to where a geothermal test well was subsequently drilled by the U. S. Bureau of Reclamation. Several sources of cultural noise are present in the area. Large fluctuations in noise level, superposed on a constant high level of noise, occur from traffic on a freeway to the south of the region. There is noise generated by canals to the west and south and agricultural activity to the west of the region. Noise at 2.5 Hz frequency generated by a small waterfall (power drop) on the All American Canal propagates as far as 10 km. Average noise levels were computed at each station using several quiet samples selected from 4-hour sections of data recorded at night and contoured. Spatial distribution of 2-3 Hz noise show noise radiating from the power drop. Noise in 0-2, 3-5, and 5-10 Hz bands show high levels extending along the freeway to the south and East High Line Canal to the west of the area. The Mesa thermal anomaly is centered about 2.5 km from the freeway and canal and does not seem to have any anomalous noise

amplitudes associated with it. Additional results using data from two arrays of closely-spaced instruments extending from the freeway to the Mesa thermal anomaly also show no indications of high noise levels over the anomaly. This conclusion differs from the results of two previous surveys in the area (Douze and Sorrells, 1972; Geothermal Staff of Teledyne-Geotech, 1972) which show well defined noise anomalies in the 0-2, and 3-5 Hz frequency bands. A search was also made for anomalous features in noise spectra and for coherent wave trains indicating the presence of discrete sources of noise. The only predominant feature in the spectra is the 2.5 Hz peak seen at most stations, from noise generated by the power drop. Records from several three-element, L-shaped arrays with 0.3 km instrument spacing show very little visual coherence. Measurements using a cross-spectral method, however, show that highly coherent waves are found at 0.4 and 2.5 Hz; coherence is less, though significant, at 3.4 and 4.4 Hz; direction studies using phase delays from the arrays give many non-unique solutions, as the array spacing is larger than the wavelengths involved. Using the knowledge that 2.5 Hz waves are generated by the power drop, the velocity of seismic noise waves in the East Mesa area is estimated to be 0.5 km/sec.

INTRODUCTION

High levels of seismic noise in the frequency range of 1-10 Hz have been reported from the vicinity of geothermal systems in New Zealand (Clacy, 1968; Whiteford, 1970), Imperial Valley, California (Douze and Sorrells, 1972; Goforth, Douze, and Sorrells, 1972), Long Valley, California (Iyer and Hitchcock, 1973), Yellowstone National

Park, Wyoming (Iyer and Hitchcock, 1974), and Surprise Valley, California (Eng and Decker, 1974). The seismic noise experiment reported here was conducted in the East Mesa area of Imperial Valley in May 1972 soon after a preliminary survey by Douze and Sorrells (1972). In August 1972 a detailed survey was completed in the area by the Geothermal staff of Teledyne-Geotech (1972) for the U. S. Bureau of Reclamation (USBR). A geothermal test well, MESA 6-1, was completed in August 1972 by USBR at approximately the center of the anomaly. The well reached a depth of 2447.5m with a bottom hole temperature of about 200° C (U. S. Bureau of Reclamation, 1973). A second test well, MESA 6-2, reaching to a depth of 1830m with bottom hole temperature of 187° C was completed in August 1973 (Swanberg, 1973).

The East Mesa is one of the few areas where openly reported results of seismic noise surveys together with test well data are available. We hope that the USGS results reported here will aid in the evaluation of seismic noise as a prospecting tool to explore geothermal systems.

EXPERIMENTAL METHODS

Slow-speed tape-recording systems with EV-17 seismometers, described by Eaton, O'Neill, and Murdock (1970), were used in the experiment. The seismometers have 1 Hz natural frequency, and the system has essentially flat response to ground velocity in the frequency range of 1-17 Hz. Ten units were used and moved around to give adequate regional coverage. Thirty-three locations were occupied to cover the survey area and at least 48 hours of recording was done at each location. The station coordinates and operation times are given in Table 1. Seventeen stations had 3 instruments

TABLE 1. Station Co-ordinates and Operation Times

Station Name	Latitude	Longitude	Start Time		Stop Time	
			Day	Time, GMT	Day	Time, GMT
BUZ	32°48'38"	115°13'42"	May 8	22h 42m	May 10	17h 30m
CAC	32°46'02"	115°12'40"	May 1	02h 01m	May 1	15h 20m
CAM	32°49'30"	115°13'42"	May 8	19h 11m	May 10	19h 06m
CEN	32°47'10"	115°14'49"	May 5	03h 35m	May 11	16h 37m
COY	32°44'11"	115°15'24"	May 5	21h 45m	May 7	18h 28m
DRA	32°48'38"	115°10'37"	May 8	23h 50m	May 10	16h 22m
GIL	32°49'16"	115°11'49"	May 6	20h 56m	May 8	17h 23m
GRE	32°46'02"	115°10'37"	May 3	02h 02m	May 3	17h 04m
GRO	32°45'09"	115°10'37"	May 6	21h 08m	May 8	18h 17m
HOR	32°44'17"	115°07'32"	May 4	19h 12m	May 6	17h 23m
LAD	32°44'17"	115°08'34"	May 6	23h 40m	May 8	17h 08m
LAN	32°50'13"	115°09'37"	April 29	09h 40m	May 11	16h 20m
LIZ	32°46'53"	115°10'37"	May 1	21h 52m	May 4	16h 44m
MES	32°45'09"	115°11'38"	May 6	19h 40m	May 7	17h 34m
MOR	32°49'30"	115°12'40"	May 7	21h 05m	May 9	21h 16m
ORA	32°47'45"	115°15'45"	May 10	02h 38m	May 11	15h 53m
OUT	32°50'33"	115°16'24"	April 27	06h 34m	April 29	15h 00m
PAL	32°46'53"	115°11'38"	May 2	03h 44m	May 2	17h 52m
PEC	32°45'09"	115°06'30"	May 5	03h 15m	May 6	21h 50m
PRA	32°46'02"	115°11'38"	April 30	22h 17m	May 2	19h 40m
RAB	32°48'38"	115°15'45"	May 10	03h 00m	May 11	15h 06m
RAT	32°46'02"	115°13'42"	April 30	22h 52m	May 3	18h 20m
ROA	32°45'09"	115°08'34"	May 3	00h 14m	May 4	20h 30m
SAG	32°49'30"	115°15'44"	May 10	00h 01m	May 10	18h 36m

Station Name	Latitude	Longitude	Start Time		Stop Time	
			Day	Time, GMT	Day	Time, GMT
SAN	32°47'45"	115°14'45"	April 27	01h 30m	April 30	16h 40m
SCO	32°46'02"	115°07'32"	May 4	00h 43m	May 5	16h 41m
SID	32°46'43"	115°12'40"	April 30	01h 38m	May 1	17h 02m
TAM	32°48'38"	115°12'40"	May 7	21h 46m	May 8	22h 30m
TAR	32°50'22"	115°13'42"	May 7	21h 40m	May 9	21h 55m
TUM	32°44'17"	115°06'30"	May 4	23h 48m	May 6	18h 26m
WAT	32°43'24"	115°14'24"	April 27	23h 46m	April 30	00h 40m
YEL	32°49'30"	115°14'45"	May 9	00h 49m	May 9	20h 00m
YUC	32°45'09"	115°07'32"	May 4	01h 28m	May 4	19h 39m

arranged in the shape of an L-array with 0.3 km instrument spacing, four stations had three-component systems, and the rest were single-component stations with vertical seismometers (Figure 1). Stations CEN near the site for MESA 6-1 and LAN in the quietest part of the area were operated continuously throughout the period of the experiment.

NOISE SOURCES IN EAST MESA

Identification of seismic noise generated by natural phenomena like geothermal systems becomes extremely difficult in the East Mesa region of Imperial Valley because many sources of cultural noise are present (Figure 1): These are,

1. The heavily travelled freeway, Interstate Highway 8.
2. East High Line Canal and the agricultural activity to the west of it.
3. All American Canal and the power drops Nos. 3 and 4.

The canals and agricultural activity seem to be continuous wide-band sources of noise. The power drop produces intense noise with seismic waves in a narrow frequency band around 2.5 Hz. The freeway, with frequent truck traffic, produces wide-band noise as well as strong amplitude variations which can be detected at distances of several kilometers from the freeway. In addition there is some contribution from wind-generated noise. We shall discuss these sources in detail in the following sections:

Freeway noise: The following discussion is based on digital analysis of vertical-component data. Four-hour data blocks (from midnight to 4 A. M. local time) were continuously digitized at 50 samples per second and root-mean-square (RMS) amplitudes were computed

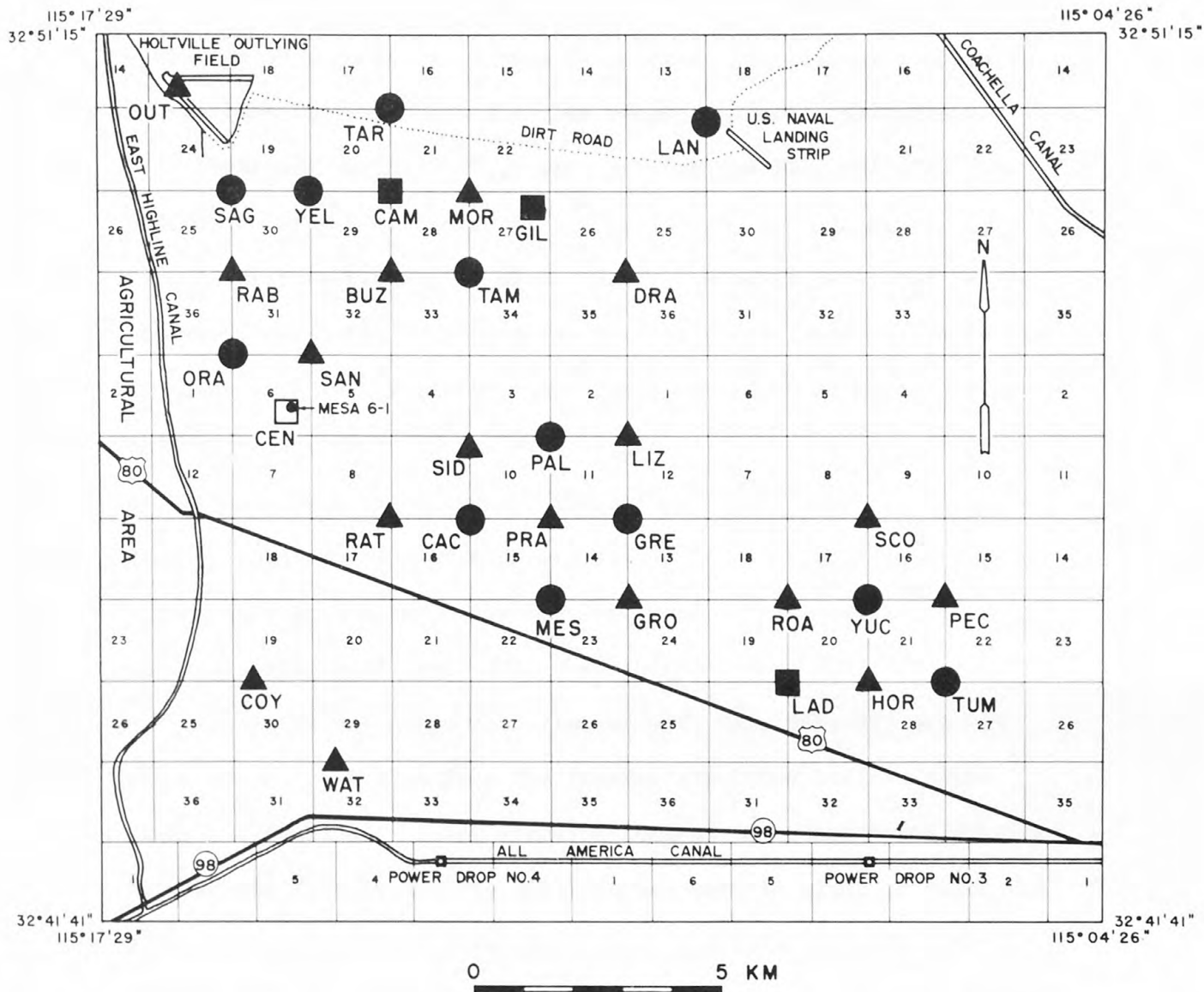


Fig. 1. Location of seismic stations occupied during the USGS noise survey in the East Mesa area of Imperial Valley. Circles indicate stations with one vertical seismometer, triangles show three-component arrays and squares indicate three-component stations. Station names are shown by 3 letters underneath the symbols. The small numerals are section numbers. The location of the USBR test well MESA 6-1 is shown near station CEN.

for every 81.92 sec (4096 points) segment. The resultant amplitude variation as a function of time was plotted for several combinations of stations for which simultaneous recordings were available.

Amplitude variation with time at stations RAT, PRA, PAL, and LIZ, which are at distances of 1.3, 2.3, 3.9, and 4.4 km, respectively, from Interstate Highway 8, show clearly the noise generated by the freeway (Figure 2). The rise and fall of noise levels at these stations are highly correlated. Amplitude varies by a factor of 13 at RAT which is closest to the freeway and a factor of 4 at LIZ which is farthest from the freeway. The quietest period at all four stations occurs around 3:10 A. M., probably due to a lull in traffic. During this period the noise level is more representative of the regional background level than when there is more traffic.

Amplitude variation with time at CEN, ORA, RAB, BUZ and SAG which are 2.5 - 6.3 km from the freeway also show traffic noise clearly (Figure 3). These stations form an important noise profile between the freeway and the MESA thermal anomaly close to where the geothermal well MESA 6-1 was subsequently drilled by USBR. At Station CEN, which is on the thermal anomaly 2.5 km from the freeway, the amplitude varies by a factor of 6. If the values of amplitude minima represent the background level of noise at these stations there is no indication that CEN has higher noise than SAG, RAB, or ORA. Note that the amplitude fluctuations as well as the mean noise level decrease with increasing distance from the freeway.

East High Line Canal Noise: Average noise levels and amplitude minima show that RAB and SAG are noisier than BUZ (Figure 3). This is explained by the fact that BUZ is farther from both the East High

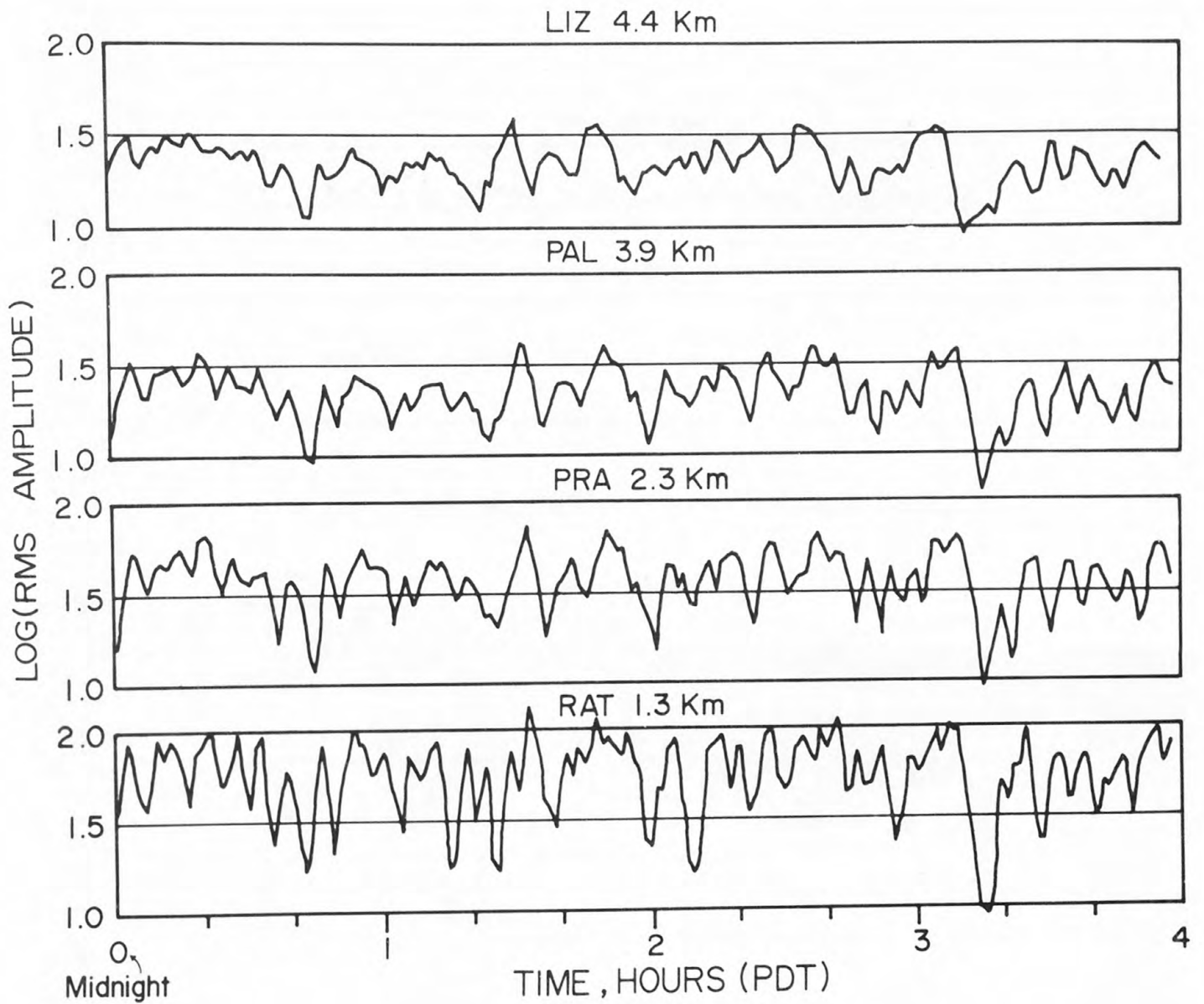


Fig. 2. Variation of seismic noise amplitude with time at stations in the central section which are at different distances from the freeway. Station names and distances from the freeway are indicated above the frame of each graph.

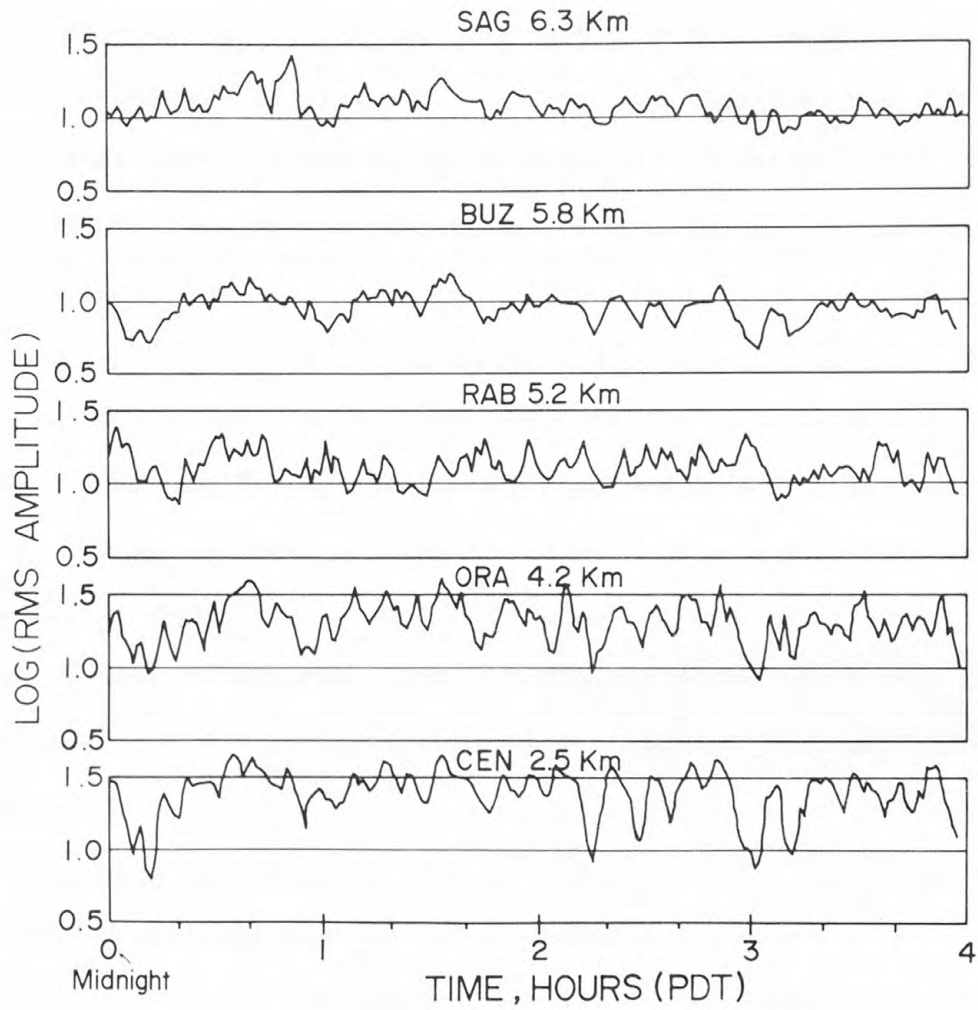


Fig. 3. Variation of seismic noise amplitude with time at stations in the western section which are at different distances from the freeway. Station names and distances from the freeway are indicated above the frame of each graph.

Line Canal (about 5 km from the canal) and the agricultural region than RAB and SAG. Simultaneous amplitude variation with time along a line extending 3 - 10 km from the East High Line Canal shows almost similar noise levels (Figure 4). We conclude therefore that the canal noise drops off rapidly with distance reaching a fairly steady level beyond 3 km, whereas the freeway effect (Figure 3) can still be seen at about 8 km.

Agricultural noise: Comparison of daytime and night time variation of noise at YEL and TAR (7 & 9 km respectively from the freeway) shows higher levels during day than during night (Figure 5). The mean level during the day is about 3 times the night level. Note the sudden drop to the night level around 12 noon at TAR and return to the mean level in about 40 minutes. This brief quiet period is clearly caused by a cessation of activity during the agricultural workers' lunch-break.

All American Canal and Power Drop No. 4 noise: Recordings at COY and WAT show the presence of a localized source of noise in the southwest section of the region. The mean noise levels at these stations are almost twice those at other stations which show high noise level. Power spectral analysis (see later section) show that the seismic waves are predominately in a narrow frequency band centered around 2.5 Hz. Geothermal Staff of Teledyne-Geotech (1972) also found this noise source and attributed it to Power Drop No. 4 (to be referred to as PD4 from now on) in the All American Canal (See Figure 1). Also, a spectral peak at 2.5 Hz can be detected at almost all the stations. Hence we think that the PD4 noise source is very strong. The narrow band-width of this noise is a fortunate

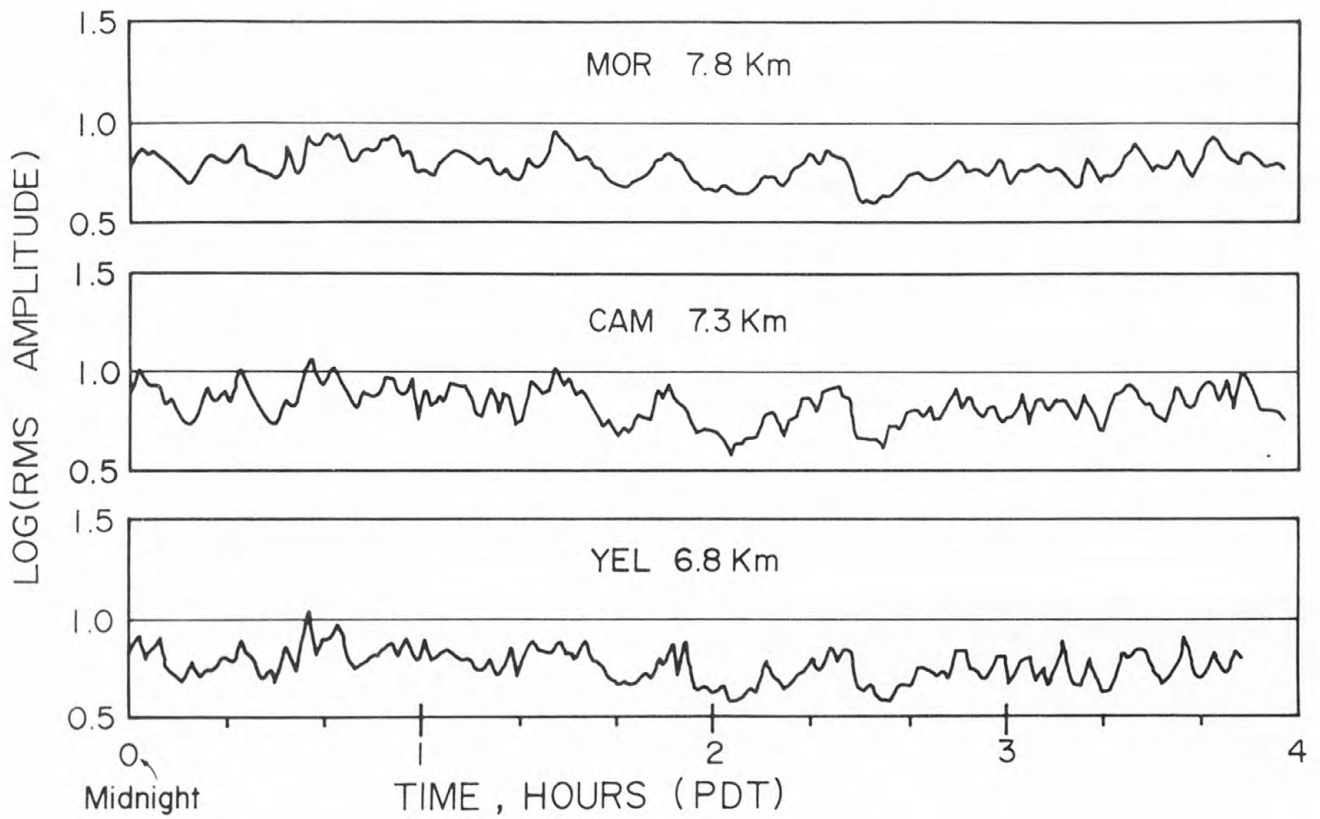


Fig. 4. Variation of seismic noise amplitude with time at stations which are more or less at the same distance from the freeway but are at different distances from the East High Line Canal. Station names and distances from the freeway are indicated above the frame of each graph. The distances of YEL, CAM, BUZ, and MOR from the canal are 3.5, 5.1, 4.8, and 6.7 km respectively.

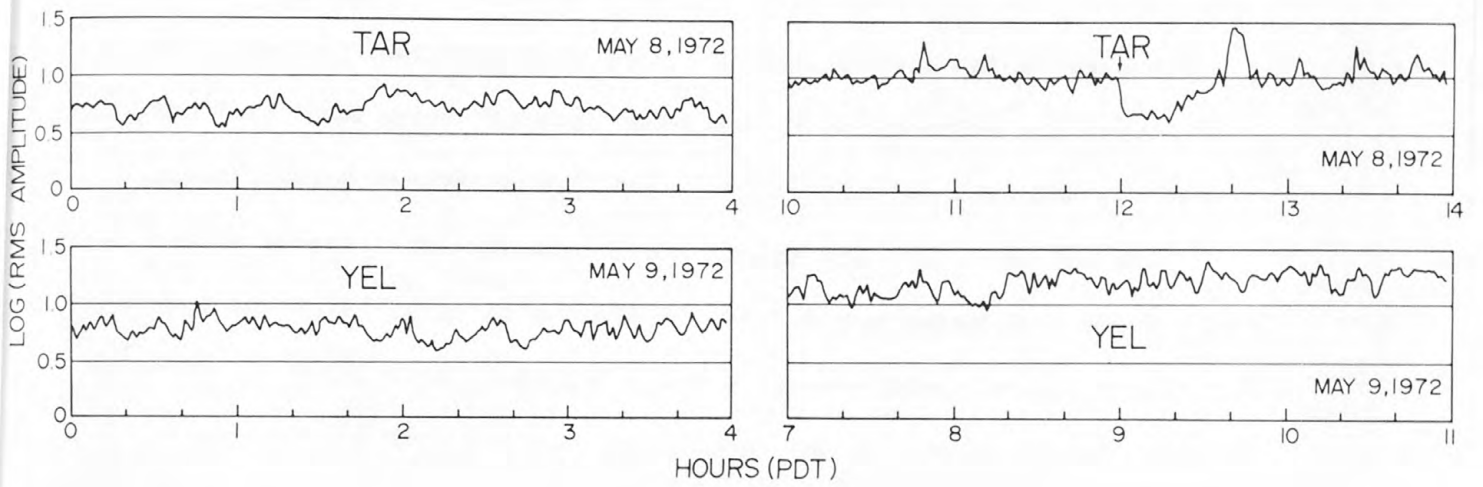


Fig. 5. Comparison of day and night noise levels at TAR and YEL. Note that the measurements at the two stations were made on different days.

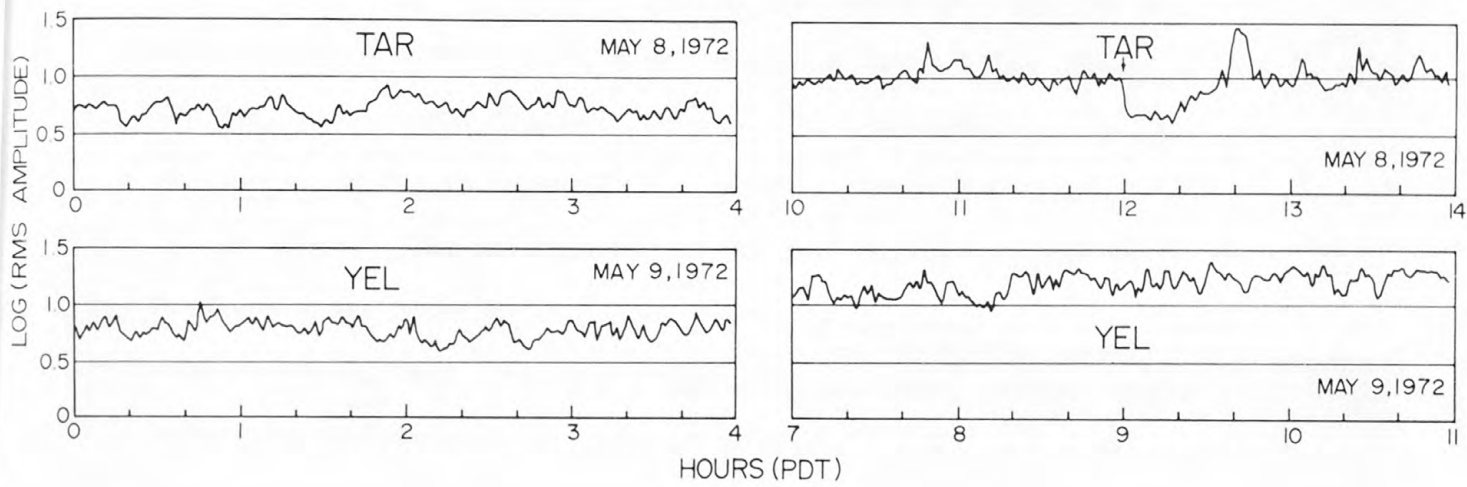


Fig. 5. Comparison of day and night noise levels at TAR and YEL. Note that the measurements at the two stations were made on different days.

circumstance as it enables filtering out this source of cultural noise. We did not operate any stations besides COY and WAT near the All American Canal and hence do not have any information on the noise generated by the canal flow.

Wind noise: The uniform geology and topography and the absence of trees provided very favorable conditions for a noise survey in the East Mesa area. Spatial variation of attenuation and ground amplification due to topographical and geological features was virtually absent. The absence of big bushes and tall trees reduced wind-generated noise to a minimum. During our experiment there were high winds and a sandstorm for about two days. Noise levels in general did not show any appreciable correlation with wind speed. As an additional safeguard our analysis is based on data recorded from midnight until 4 A. M. when wind-speed was less than 10 knots except during the wind storm when the speed was 15 knots for two nights (See Figure 6). The wind data is from El Centro Airport which is about 30 km from the East Mesa area.

Variation of regional noise during the experiment: In addition to locally generated noise there is always some regional background noise present. This could be oceanic microseisms (Haubrich, 1967) and seismic noise generated by wave action on large bodies of water. Usually the contribution from these sources at frequencies above 1 Hz is quite small, but during a storm there could be considerable increase in the regional level. In a noise survey, different points in an area are surveyed at different times, and hence a significant change in regional noise level can lead to erroneous interpretation. To safeguard against this eventuality, Stations CEN and LAN were

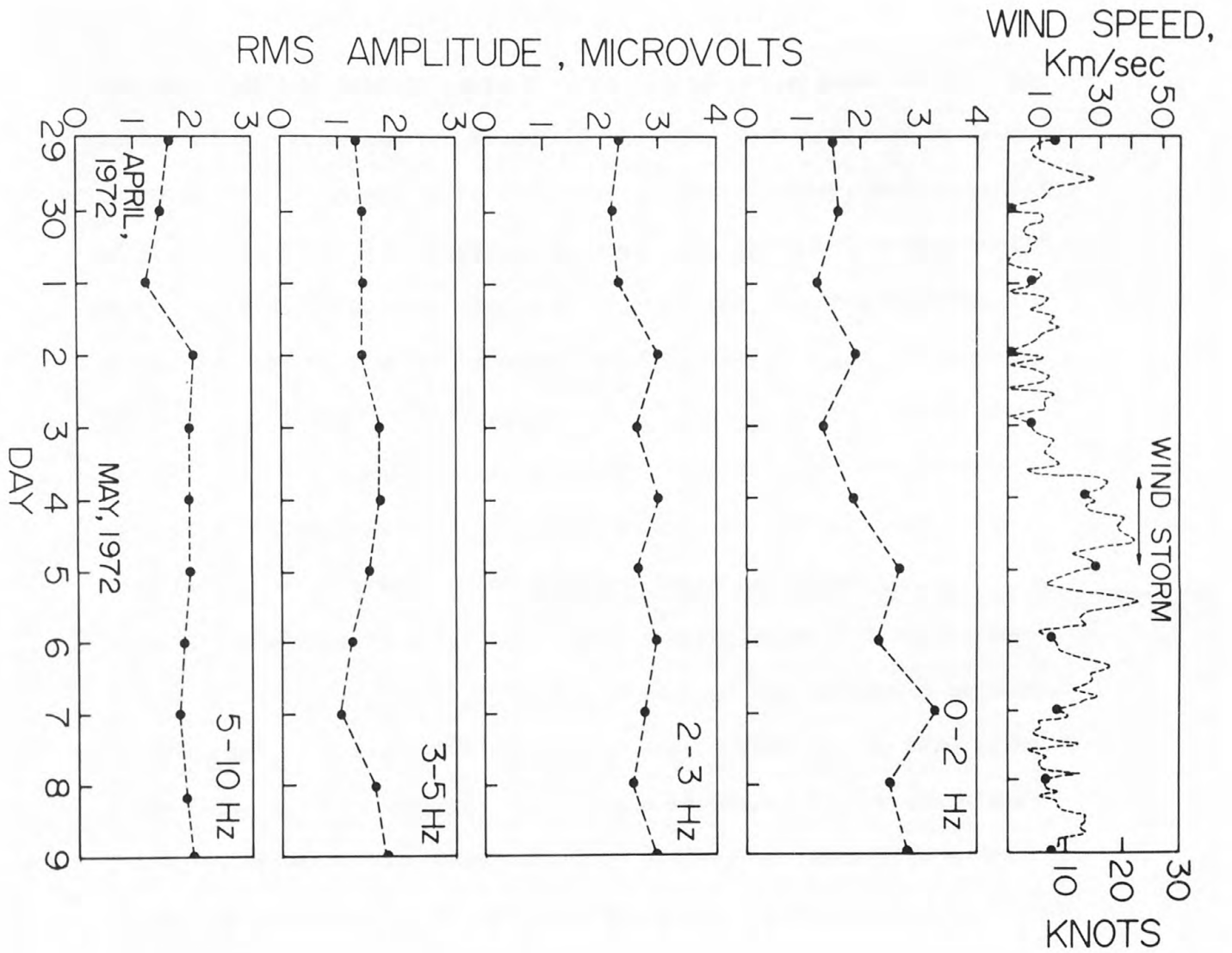


Fig. 6. Variation of noise level in different frequency bands at LAN during the period of the experiment. The top curve shows the variation of wind speed at El Centro airport using hourly readings (Courtesy of U. S. Weather Bureau, El Centro, California). The dots correspond to times at which noise samples were taken.

operated continuously to monitor variation of noise level during the period of our experiment. Since CEN was very much affected by freeway noise it was not possible to evaluate realistically the daily variation of noise level at that station. However, the amplitude minima at CEN showed little change from day to day indicating that the regional background level of noise remained fairly constant. LAN, located on the east landing strip (Figure 1), about 10 km from the freeway and agricultural area, was a quiet station. Average noise amplitudes for several frequency bands were computed using 10 samples of digitized data (40.96 sec blocks) around midnight every day (Figure 6). No significant change in noise level was observed above 2 Hz. The low frequency noise below 2 Hz, however, increased and reached a maximum of twice the original value during the last 5 days of the experiment. Since this increase occurred following a severe windstorm the higher noise levels might have been caused by microseisms from high waves in the Salton Sea, which is about 60 km to the northwest of LAN. Since it takes a finite time for sea waves to build up and high wave amplitudes persist and are sustained by wind even after a wind storm is over, it is not surprising that the noise level continued to be high for several days.

SPATIAL VARIATION OF NOISE

It is clear from the previous section that, except in very special cases, contouring of seismic noise levels using one short sample record per location can lead to erroneous results. The general belief that seismic noise is a simple tool in geothermal prospecting is questionable.

In this section several ways of evaluating and presenting spatial variation of background noise in the East Mesa area will be discussed. The analysis is based on 4-hour blocks of digitized data from midnight until 4 A. M. local time.

Evaluation of average noise amplitude. The first step is to estimate a realistic average noise level at each location. In their survey at East Mesa, Goforth, Douze, and Sorrels (1972) averaged ten 200-second segments from 8 hours of night recording, making certain that no obvious cultural noise transients were included in the segments. In the second survey, the Geothermal Staff of Teledyne-Geotech (1972) used 28 short segments (10.04 sec) from 12 hours of recording to compute average noise. The samples were carefully chosen to exclude transient signals caused by earthquakes and road traffic. In the present analysis, to reduce any subjective bias in selection, 4-hour digital data blocks were divided into 175 continuous 81.92 sec segments, and 10-20 of the quietest blocks were used for calculating average noise levels.

RMS amplitudes were computed for all segments. Averages of 20 quietest values (\bar{a}) together with standard deviations are given in Table 2. The noise levels are measured in ground velocity units of millimicrons/sec ($m\mu$ /sec) which is the same as nanometers/sec used by Geothermal Staff of Teledyne-Geotech (1972). The average amplitude in logarithmic scale when plotted as a function of distance from the freeway shows a linear relationship (Figure 7) indicating a simple law of exponential decay. Note that the standard deviations are in general high near the freeway showing that large fluctuations in noise level occur as the freeway is approached. The results show that in

TABLE 2. Average Noise Amplitudes Using Unfiltered Data

Station	\bar{a} m /sec	Standard Deviation	$\bar{P}=20 \text{ Log}_{10}(\bar{a})$ db	Distance from Freeway, km
BUZ	82.0	7.1	38.3	5.8
CAC	195.2	31.1	45.8	1.8
CAM	69.3	5.2	36.8	7.3
CEN*	147.1	31.3	43.4	2.5
COY	227.7	6.5	47.1	2.6
DRA	117.4	6.8	41.4	7.4
GIL	69.3	2.5	36.8	8.0
GRE	165.5	30.6	44.4	2.9
GRO	203.7	42.4	46.2	1.4
HOR	237.6	67.6	47.5	1.6
LAD	230.6	47.1	47.3	1.0
LAN	52.3	2.0	34.4	10.6
LIZ	158.4	24.9	44.0	4.4
MES	247.5	16.4	47.9	0.8
MOR	67.9	3.3	36.6	7.9
ORA	161.2	23.2	44.1	4.2
OUT	127.3	3.3	42.1	6.5-8.0
PAL	165.5	29.4	44.4	3.9
PEC	108.9	16.5	40.7	3.6
PRA	210.7	39.6	46.5	2.3
RAB	121.6	8.6	41.7	5.2
RAT	268.1	66.1	48.6	1.3

TABLE 2 (Cont'd)

Station	\bar{a} m /sec	Standard Deviation	$\bar{P}=20 \text{ Log}_{10}(\bar{a})$ db	Distance from Freeway, km
ROA	157.0	36.6	43.9	2.5
SAG	126.4	7.6	42.0	6.3
SAN	87.7	8.5	38.9	3.8
SCO	110.3	9.1	40.9	4.6
SID	154.2	13.9	43.8	3.3
TAR	55.2	3.3	34.8	8.9
TUM	188.1	42.3	45.5	2.1
WAT	216.4	3.1	46.7	3.6
YEL	63.6	4.0	36.1	6.8
YUC	148.5	25.5	43.4	3.0

*This station is near the center of Mesa thermal anomaly.

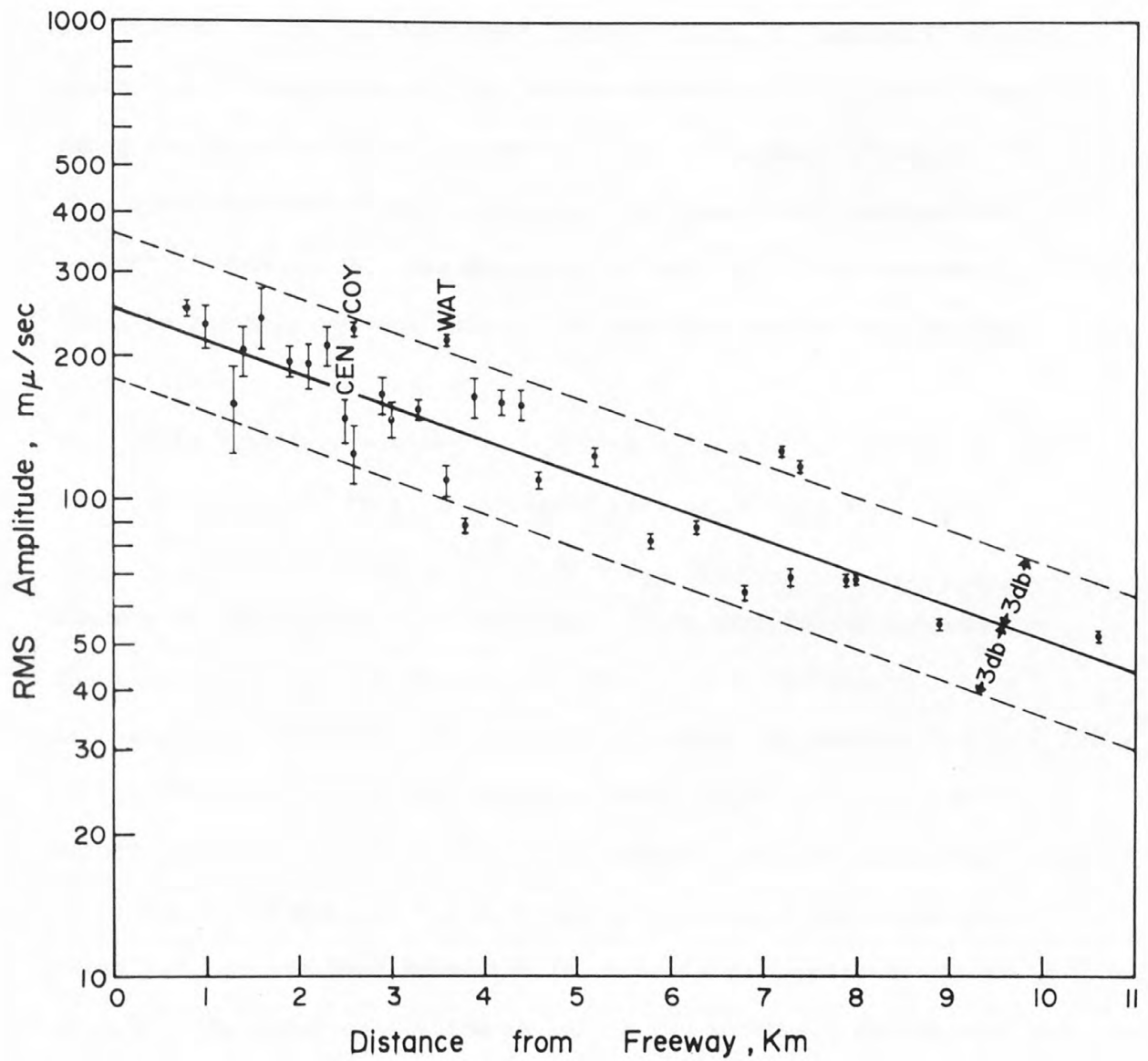


Fig. 7. Variation of average noise level with distance from the freeway. The solid line indicates the average trend and the dashed lines show 3 db variation from this average. The bar denotes one standard deviation of the average value.

addition to amplitude fluctuations the freeway produces a constant noise level. From the amplitude distance graph, Q (anelastic attenuation) can be calculated. For a wave velocity of 0.5 km/sec (see later section) Q works out to about 7 for a frequency of about 3 Hz. In general the individual values fit this attenuation pattern with a scatter of about 3 db. The stations CEN and SAN, which are very close to the Mesa thermal anomaly, do not show any abnormally high noise levels.

These results are shown as contours of spatial variation of noise power in Figure 8. Power in decibels (db) is defined as follows:

$$P = 10 \text{ Log}_{10} (\bar{a})^2 = 20 \text{ Log}_{10} (\bar{a})$$

where \bar{a} is the average RMS amplitude. (Note that in our computation power is defined as the mean-square amplitude of the record. If a_n is the digital amplitude and N the total number of samples, $P = \frac{1}{N} \sum_{n=1}^N 1/2 a_n^2$. In the Teledyne-Geotech work power spectral estimates were made by the method described by Welch (1967). To make the two estimates comparable 12 db has to be added to Teledyne-Geotech values). The variation of noise level in the East Mesa area is about 13 db (amplitude change by a factor of 4.5). The quietest station is LAN in the northeast corner near the (abandoned) U. S. Naval Landing Strip. Highest noise levels occur along the freeway and East High Line Canal. A northeast trending anomaly extends from the freeway and is caused by the 2.5 Hz seismic noise generated by PD4 (see below). No localized noise anomaly is seen in the area of the Mesa thermal anomaly marked by MESA 6-1 in the figure. (Note that due to digitizing problems data from TAM was not used in any of the computations).

Average noise amplitudes and power were computed for different frequency bands using 10 quietest segments of data selected from 4-hour

UNFILTERED

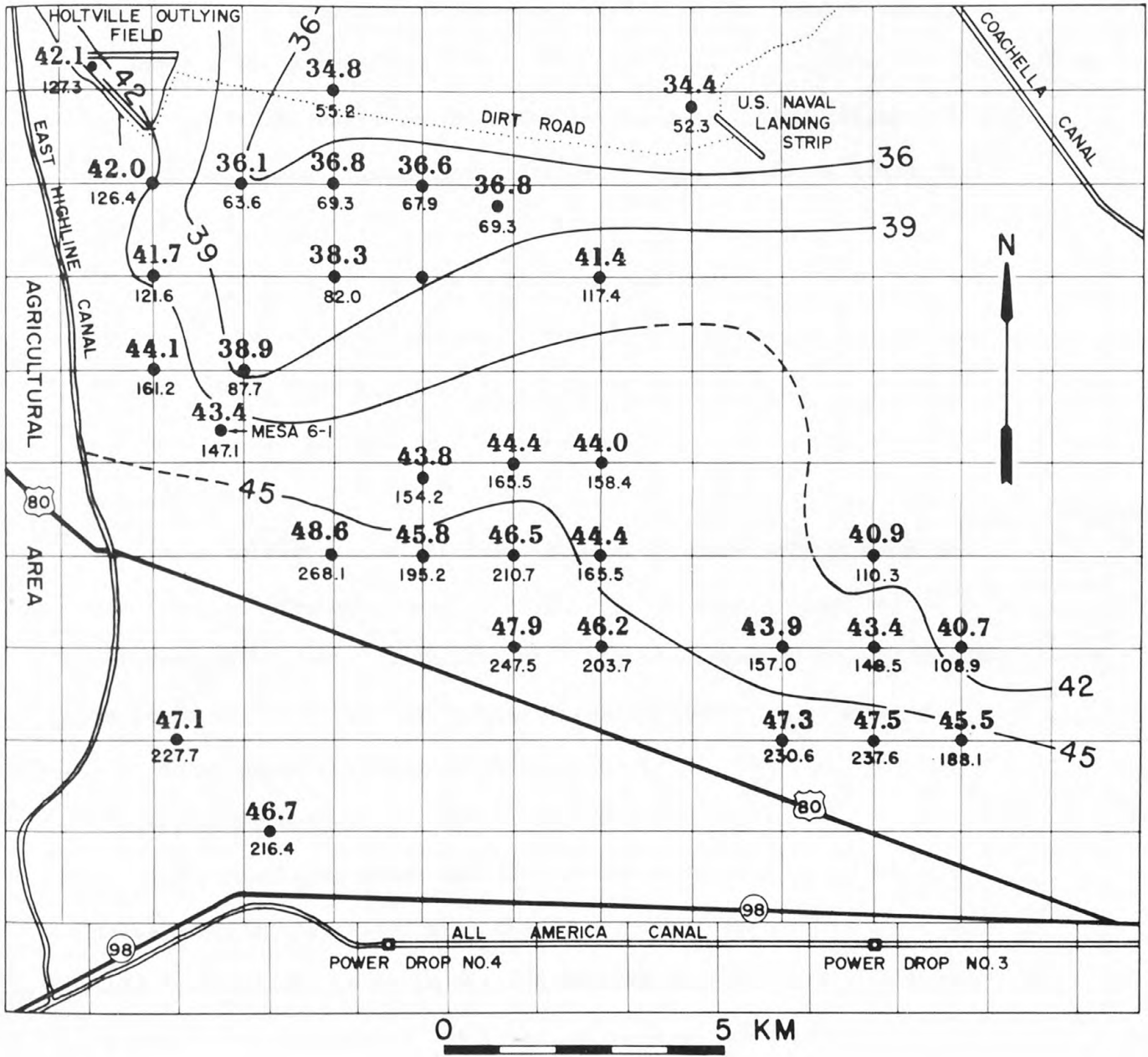


Fig. 8. Spatial variation of unfiltered noise level in the East Mesa area. Noise power in db is shown above the dot which indicates station location and the corresponding RMS amplitude in millimicrons/sec is shown below the dot. The contour interval is 3 db.

records. Each data segment was band-pass filtered and average RMS amplitude and power computed as discussed earlier. The results are given in Table 3 and Figures 9-12.

The spatial variation of noise in the 0-2 Hz band (Figure 9) does not show anything significantly different from the total noise field discussed earlier.

The contours for 2-3 Hz noise show mainly the effect of a noise source in the southwest corner (Figure 10) superimposed on canal and freeway noise. The most likely source of this noise is PD4. The attenuation seems to be less in a northeasterly direction than towards north and northeast.

Results for the 3-5 Hz band (Figure 11) show only freeway and canal noise. The noise high in Figure 11 is to the southeast of MESA 6-1, and is probably associated with higher frequency noise from PD4. Hence we do not attach any special significance to this anomaly.

Noise power contours in the 5-10 Hz band (Figure 12) are not significantly different from the 3-5 Hz band (Figure 11).

In summarizing these results, we conclude that we do not see a noise anomaly associated with the Mesa thermal anomaly in any frequency band. If seismic noise in the 3-5 Hz band is generated by a hydrothermal source under the anomaly the level is clearly less than the cultural noise in the area. Our results show significant deviation from the results of Goforth and Douze (1972) and the Geothermal Staff of Teledyne-Geotech (1972). Goforth and Douze (1972) show the presence of a noise anomaly of about 3 km diameter over the Mesa thermal anomaly. Results of Geothermal Staff of Teledyne-Geotech (1972) show a northeast trending noise anomaly extending from the freeway through MESA 6-1 in

TABLE 3. Average Noise Amplitudes in Different Frequency Bands

Station	0-2 Hz		2-3 Hz		3-5 Hz		5-10 Hz	
	a m μ /sec	p db	a m μ /sec	p db	a m μ /sec	p db	a m μ /sec	p db
BUZ	33.9	30.6	38.2	31.6	38.2	31.6	33.9	30.6
CAC	45.3	33.2	141.4	43.0	94.8	39.6	70.7	37.0
CAM	35.4	31.0	33.9	30.6	32.5	30.2	25.5	28.2
CEN*	38.2	31.6	82.0	38.2	63.6	36.0	43.8	32.8
COY	66.5	36.4	195.2	45.8	55.2	34.8	48.1	33.6
DRA	45.3	33.2	75.0	37.6	46.7	33.4	43.8	32.8
GIL	25.5	28.2	48.1	33.6	22.6	27.0	28.3	29.0
GRE	25.5	28.2	79.2	38.0	76.4	37.6	63.6	36.0
GRO	62.2	35.8	59.4	35.4	65.1	36.2	90.5	39.2
HOR	48.1	33.6	60.8	35.6	73.5	37.4	69.3	36.8
LAD	60.8	35.6	82.0	38.2	110.3	40.8	65.1	36.2
LAN	19.8	26.0	32.5	30.2	19.8	26.0	19.8	26.0
LIZ	39.6	32.0	90.5	39.2	96.2	39.6	69.3	36.8
MES	46.7	33.4	155.6	43.8	53.7	34.6	82.0	38.2
MOR	25.5	28.2	41.0	32.2	24.0	27.6	21.2	26.6
ORA	43.8	32.8	79.2	38.0	80.6	38.2	60.8	35.6
OUT	59.4	35.4	79.2	38.0	55.2	34.8	52.3	34.4
PAL	35.4	31.0	79.2	38.0	77.8	37.8	55.2	34.8
PEC	31.1	29.8	46.7	33.4	52.3	34.4	49.5	33.8
PRA	36.8	31.4	97.6	39.8	113.2	41.0	59.4	35.4

Station	0-2 Hz		2-3		3-5		5-10	
RAB	39.6	32.0	66.5	36.4	72.1	37.2	38.2	31.6
RAT	33.9	30.6	94.8	37.6	89.1	39.0	55.2	34.8
ROA	38.2	31.6	67.9	36.6	75.0	37.6	66.5	36.4
SAG	50.9	34.2	58.0	35.2	75.0	37.6	55.2	34.8
SAN	31.1	29.8	46.7	33.4	46.7	33.4	28.3	29.0
SCO	36.8	31.4	60.8	35.6	60.8	35.6	39.6	32.0
SID	33.9	30.6	120.2	41.6	104.7	40.4	60.8	35.6
TAR	29.7	29.4	29.7	29.4	22.6	27.0	18.3	25.2
TUM	35.4	31.0	56.6	35.0	79.2	38.0	62.2	35.8
WAT	35.4	31.0	188.1	45.4	69.3	36.8	50.9	34.2
YEL	31.1	29.8	33.9	30.6	26.9	28.6	25.5	28.2
YUC	39.6	32.0	65.1	36.2	66.5	36.4	52.3	34.4

*This station is near the center of Mesa Thermal anomaly.

0 - 2 HZ

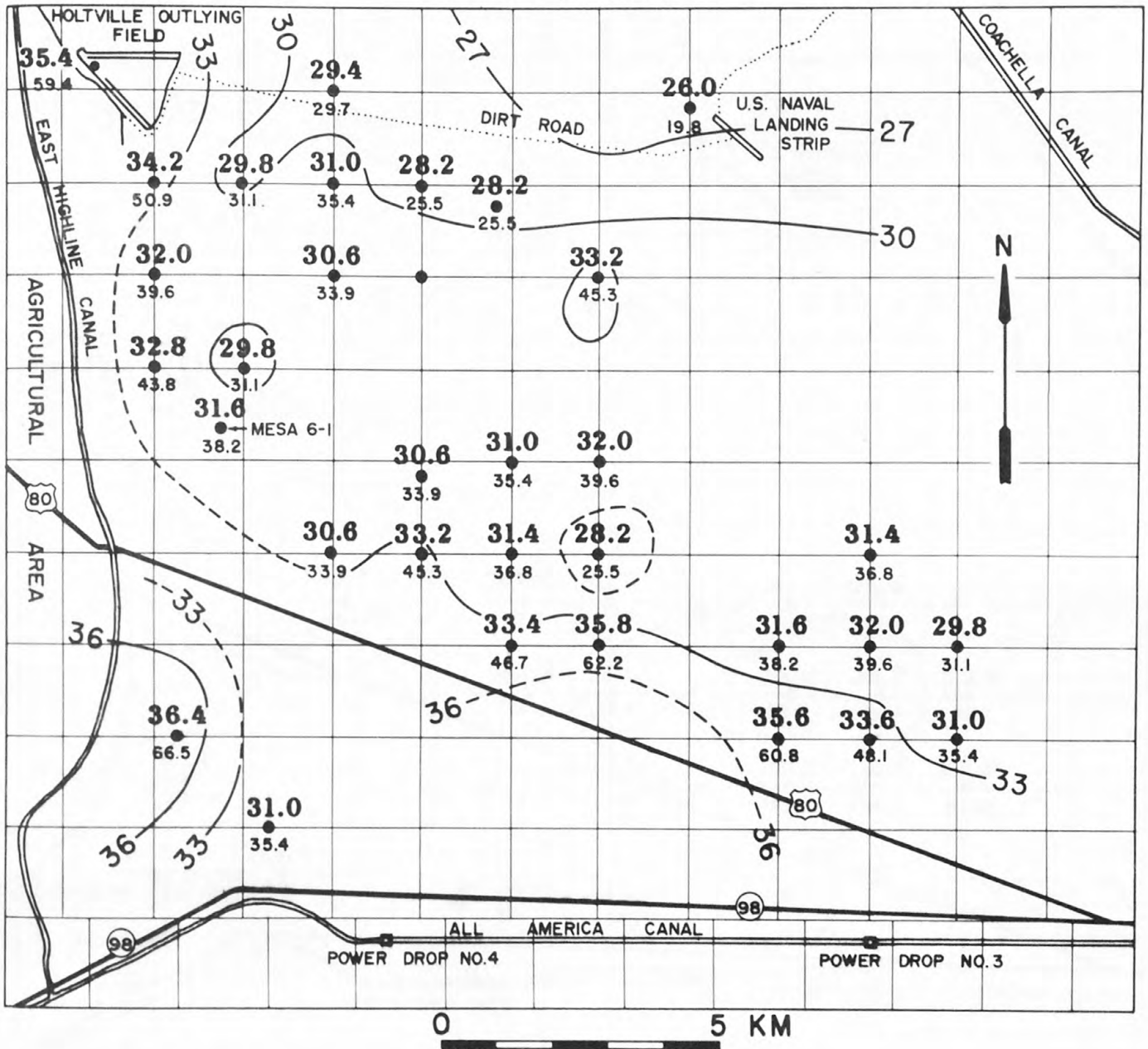


Fig. 9. Spatial variation of 0-2 Hz noise level in the East Mesa area. Noise power in db is shown above the dot which indicates station location and the corresponding RMS amplitude in millimicrons/sec is shown below the dot. The contour interval is 3 db.

2 - 3 HZ

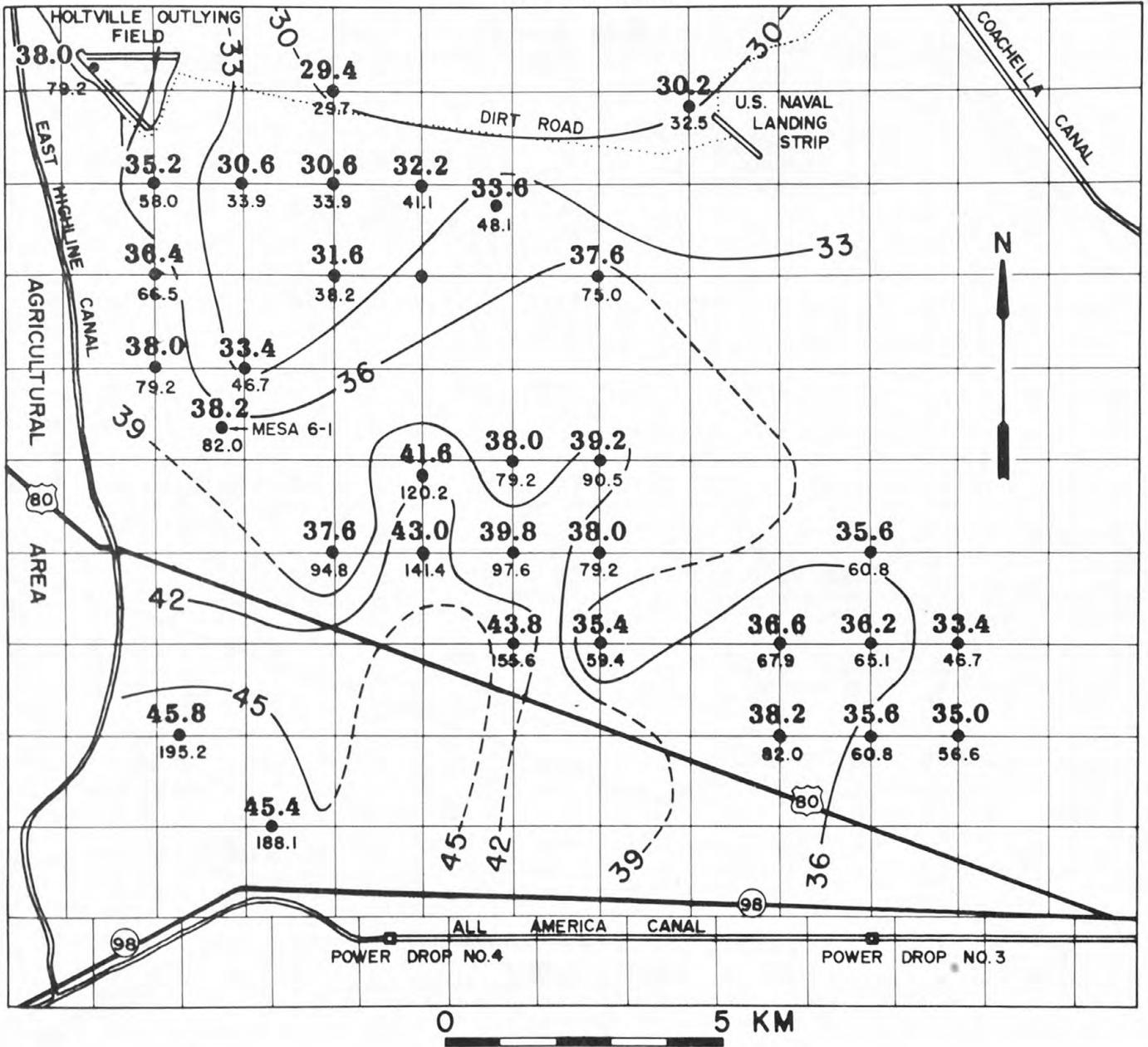


Fig. 10. Spatial variation of 2-3 Hz noise level in the East Mesa area. Noise power in db is shown above the dot which indicates station location and the corresponding RMS amplitude in millimicrons/sec is shown below the dot. The contour interval is 3 db.

3 - 5 HZ

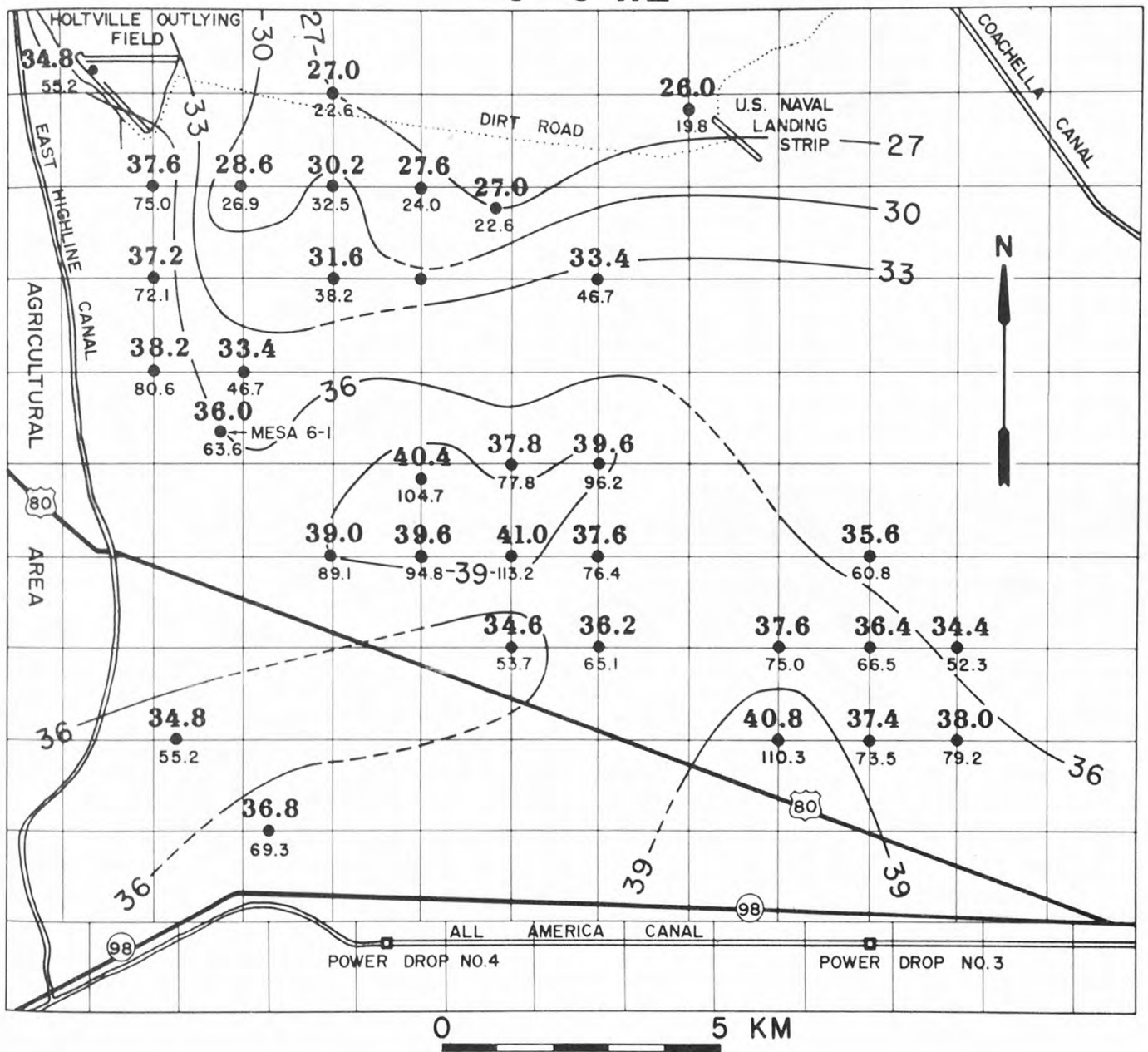


Fig. 11. Spatial variation of 3-5 Hz noise level in the East Mesa area. Noise power in db is shown above the dot which indicates station location and the corresponding RMS amplitude in millimicrons/sec is shown below the dot. The contour interval is 3 db.

5 - 10 HZ

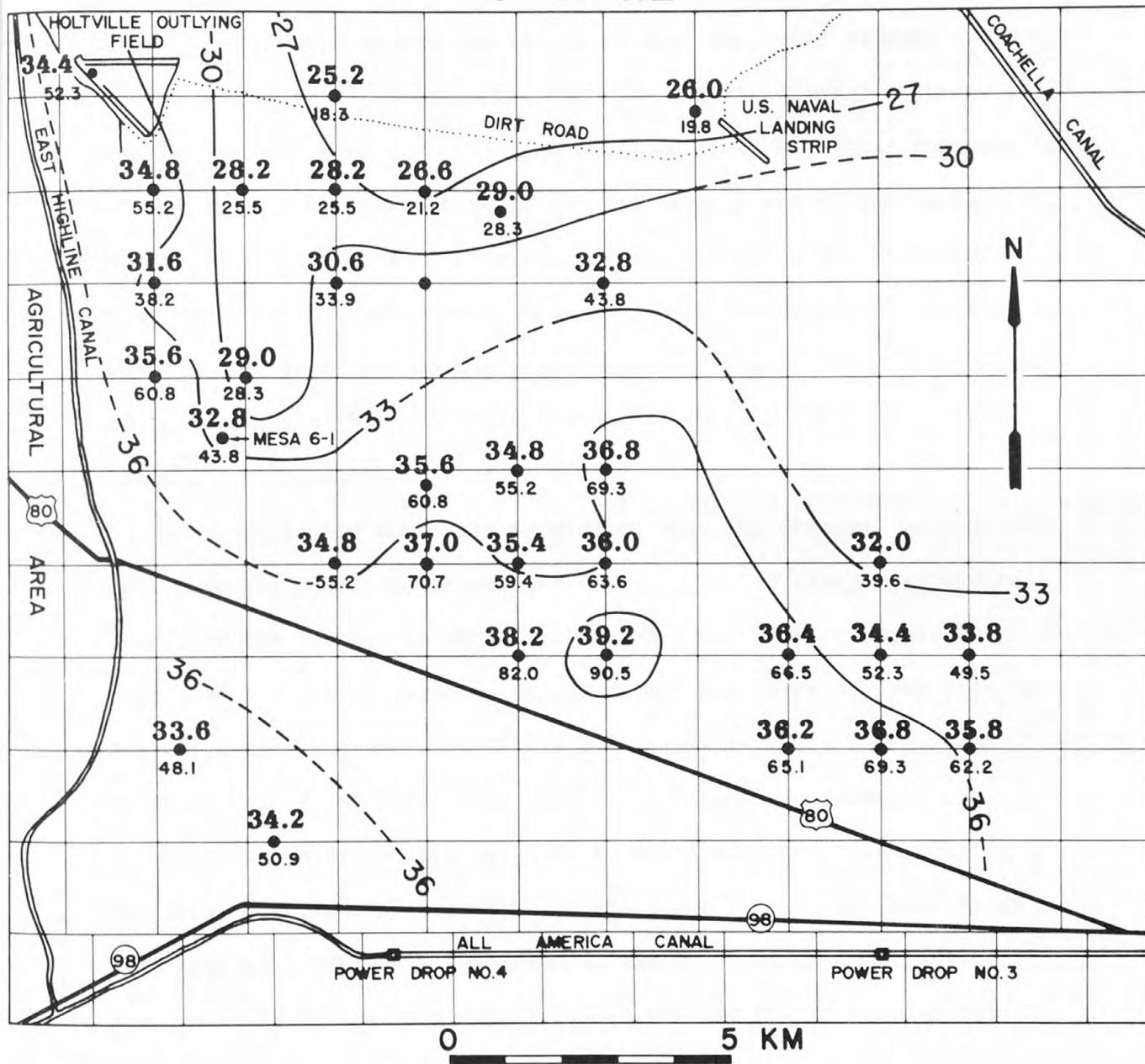


Fig. 12. Spatial variation of 5-10 Hz noise level in the East Mesa area. Noise power in db is shown above the dot which indicates station location and the corresponding RMS amplitude in millimicrons/sec is shown below the dot. The contour interval is 3 db.

the frequency bands, 1-2 Hz, and 3-5 Hz. Note from Figure 11 that the cultural noise level near MESA-6-1 is 36 db and is higher than the level at the quietest station LAN by 10 db. The noise anomaly found by Geothermal Staff of Teledyne-Geotech (See Figures 4 and 5 of their 1972 report) is only 1 km wide and 3 km long and 12-15 db higher than the level at the quiet stations. It seems to rise clearly out of the background noise. Noise levels at the Teledyne-Geotech Station 20, near the peak of the anomaly, is higher than the level at Station 32, outside the anomaly, by 6 db. On the other hand, our Station CEN which corresponds to Teledyne-Geotech Station 20 has 3 db less noise power than RAT which corresponds to Station 32.

To make doubly sure that we did not miss the anomaly, we analyzed data from three seismic arrays which were operated along the service road from the freeway to MESA 6-1. Array A had 6 instruments, A1 to A6, connected by wire to a recording truck, and was operated from 7:45 to 9:15 A. M. local time; array B had 8 instruments B1 to B8, and was operated 9:30 P. M. until midnight; array C had 6 instruments C1 to C6 and was operated from 9:45 P. M. until midnight (Figure 13). The three measurements were done on different days. The location of USBR test well MESA 6-1 is between B2 and B3. Ten quietest noise samples of 40.96 sec were digitized and average RMS amplitudes computed for various frequency bands.

The average noise level in the 3-5 Hz band, when plotted as a function of distance from the freeway (shown by dots with error bars in Figure 14), show very little variation. Note that the average noise amplitudes as measured using the USGS arrays are about 12 db higher than the estimated level of 36 db at CEN. To resolve this,

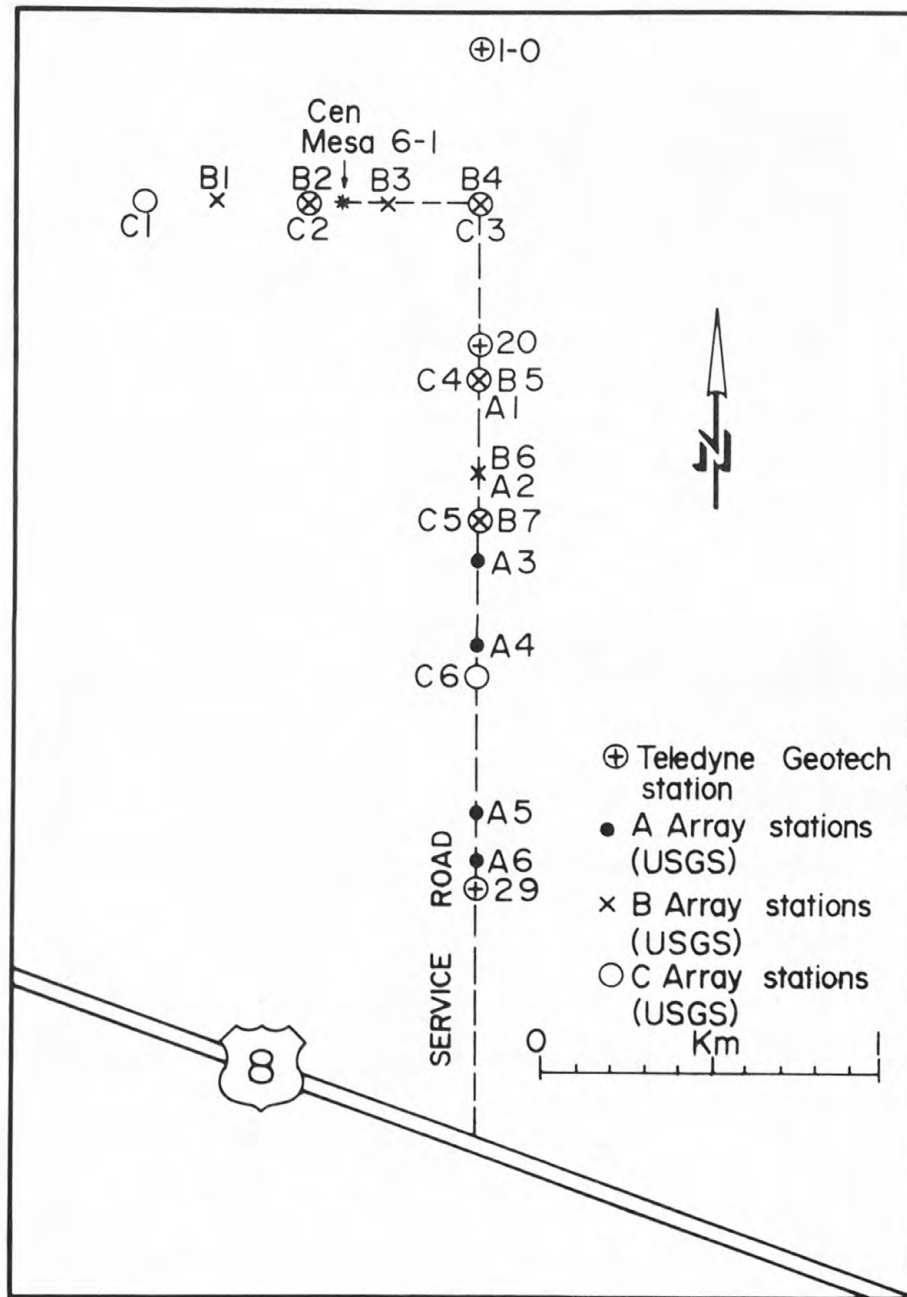


Fig. 13. Location of instruments in the two short-term arrays which were operated to measure seismic noise across the Mesa thermal anomaly. The location of three Teledyne-Geotech stations are also shown. (See Geothermal staff of Teledyne-Geotech, 1972).

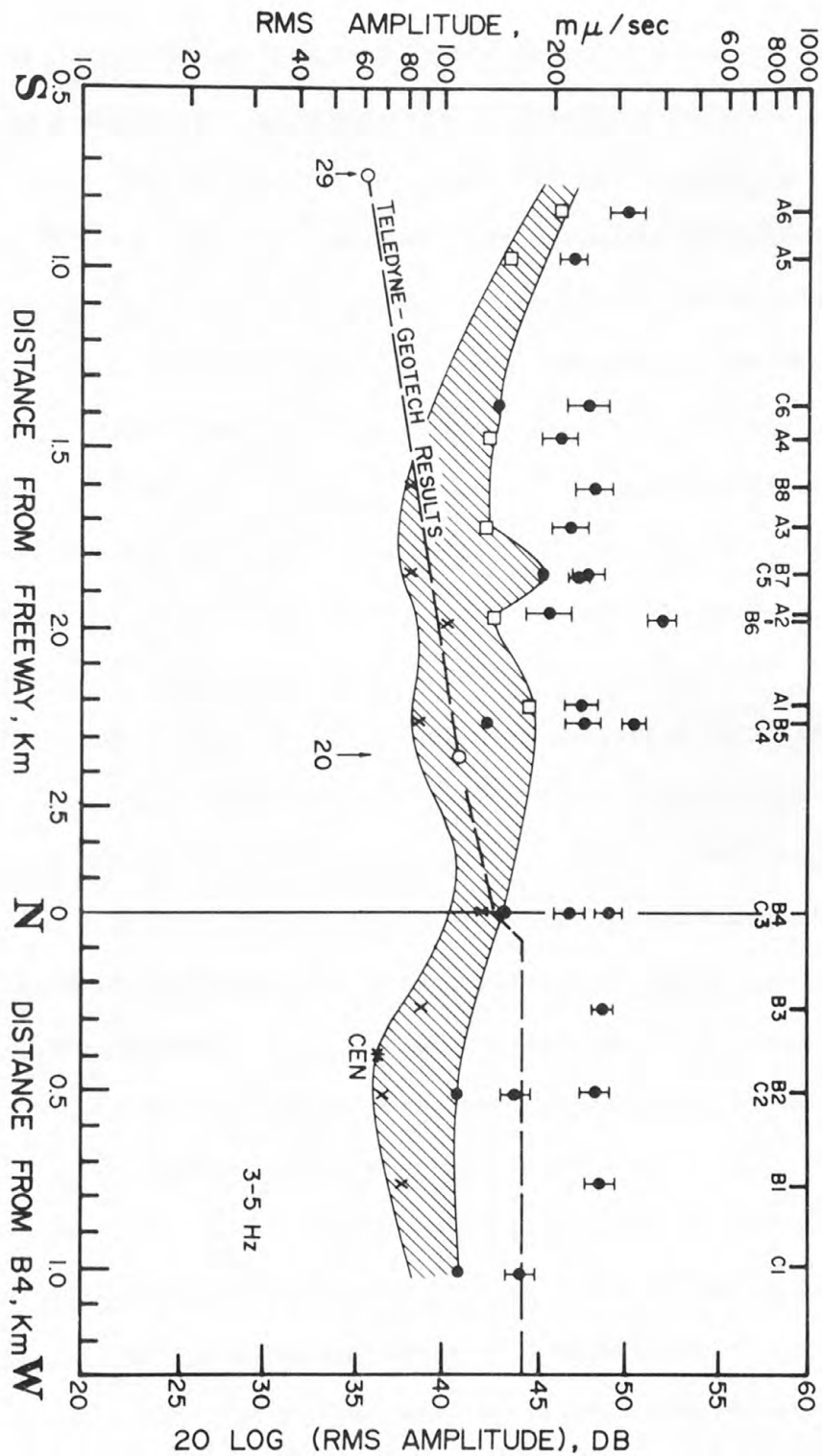


Fig. 14. Variation of 3-5 Hz noise from the freeway to the Mesa thermal anomaly. The USGS station names are shown along the top and the noise levels by dots. The vertical lines indicate one standard deviation. The Teledyne-Geotech results (12 db added) are shown by circles and the station names are indicated below them. The dashed line, which represents variation of Teledyne-Geotech noise level, is based on measurements at stations 29, 20, and 1-0 between the freeway and B4 and their noise contours from B4 towards west. (See Geothermal Staff of Teledyne-Geotech, 1972). The average noise level at CEN and the quietest noise amplitudes recorded by the three arrays are shown by the various symbols in the shaded area. (Squares - Array A, crosses - Array B, solid circles - Array C).

the lowest noise levels recorded by the arrays were estimated by digitally scanning the recorded data as described earlier. These values (shown within the shaded area in Figure 14) are comparable to the noise level at CEN. It appears therefore that estimates of noise levels based on averaging ten quiet samples is dominated by the traffic noise on the freeway. The quietest noise levels represent the best estimate that can be made of non-cultural noise. The width of the shaded area in Figure 14 shows the extent of scatter in the measurements (3-5 db).

Teledyne-Geotech results (also shown in Figure 14) show a 9 db increase in noise level between the freeway and the peak of the thermal anomaly near MESA 6-1. Up to a distance of about 1.5 km north from the freeway the USGS (quietest) values are clearly higher than the expected levels from Teledyne-Geotech measurements. From 1.5-2.8 km the two estimates agree more or less. Along the section from B4 towards west, where the thermal and Teledyne-Geotech noise anomalies reach maximum values, the USGS measurements are lower by 3-6 db. The agreement between USGS and Teledyne-Geotech results is therefore poor and if a noise anomaly is present at East Mesa it is barely discernible by our experiment.

We are unable to give any clear explanation for the difference between USGS and Teledyne-Geotech results. The following possibilities are listed in decreasing order of probability:

1. Since the area is dominated by time-varying freeway noise there are bound to be differences in choice of quiet periods for analysis leading to ambiguities in determining the average noise level.
2. The geothermal system was more active during the Teledyne-Geotech experiments and was quieter during our experiment.

3. The anomaly existed but was missed by USGS experimental and analysis procedures.

SPECTRAL STUDIES

Power spectra were computed using 40.96 sec data blocks, digitized at 50 samples per second using the Fast Fourier Transform. A 15-point triangular window was used to smooth the spectra. Usually two spectra were computed using data recorded at night corresponding to lowest and highest noise levels. The normalization of the spectrum is such that its integral over frequency is equal to the mean-square amplitude (see earlier section for details).

Spectra for a group of six stations near the western boundary of East Mesa area show that the seismic energy is mainly concentrated in the frequency band of 2-6 Hz for the quiet periods and the noisy intervals (Figure 15). Thus it appears as if this frequency band corresponds to the preferential mode of excitation of the ground in the East Mesa area. Note that the difference between the high and low noise spectra is highest in this frequency band at all stations. This is because the excitation of the ground by cultural noise sources, like traffic, generates higher amplitude seismic waves in the 2-6 Hz band than at other frequencies. Except at RAT near the freeway there is virtually no difference between the high and low noise spectra below 2 Hz. The spectrum of the low noise block at CEN, on the top of the MESA thermal anomaly, is not significantly different from corresponding spectra at the other stations. It is thus clear that there are no indications for the presence of geothermal noise with identifiable spectral characteristics under the MESA thermal anomaly.

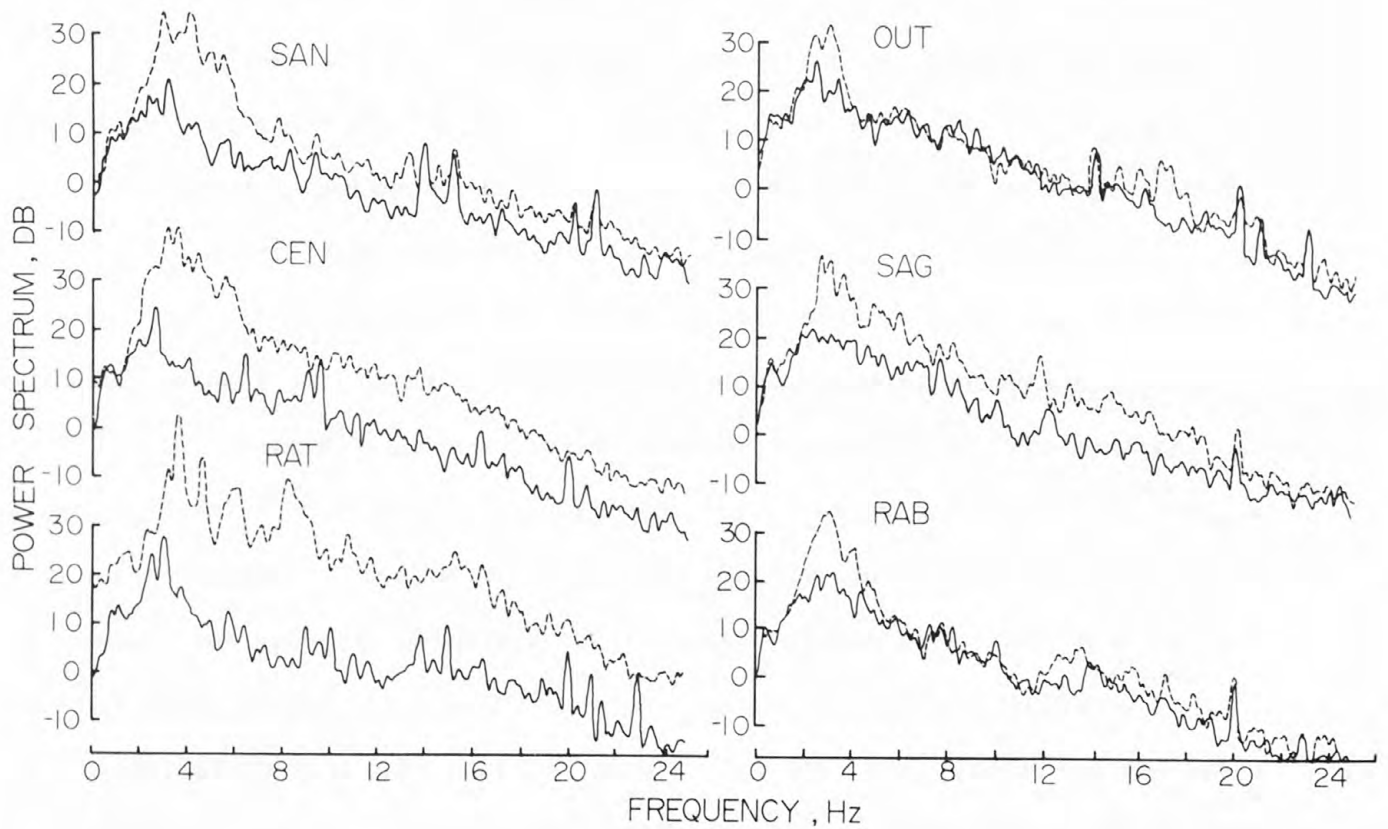


Fig. 15. Noise spectra at stations along the western section of the East Mesa area. The dashed and solid lines show spectra of highest and lowest levels of noise during a four-hour recording period from midnight to 4 a.m.

Noise spectra for a group of six stations near the northern boundary of the East Mesa area (distances greater than 6 km from the freeway) show that the general spectral shape and the difference between high and low spectra are almost the same at all the stations (Figure 16). There seems to be a spectral peak near 8 Hz at these stations (clearly seen at LAN). We are unable to attach any special geothermal significance to this peak.

The propagation of the seismic noise in the 2-3 Hz band, generated by PD4 across the whole area of the experiment is demonstrated by the low noise spectra at two groups of stations (Figures 17a and 17b). WAT shows a pronounced peak at 2.5 Hz and is used as reference station for the spectral sections towards northeast and north. This spectral peak can be seen at all the stations. A secondary peak near 3 Hz can also be seen at most of the stations. Neither of the peaks shows a clear-cut case for attenuation with distance from the source which is close to WAT. It is probable that these spectral peaks (to be referred to as 2.5 Hz peaks in future) are the normal modes for surface wave propagation and are fortuitously excited by favorable characteristic frequency of canal turbulence associated with PD4.

In summarizing we find that the shapes of seismic noise spectra in the East Mesa area do not reveal any information on the presence or absence of geothermal noise sources.

COHERENCE AND DIRECTION STUDIES

As mentioned earlier, several L-shaped arrays were operated during our experiment. Each array had 3 vertical seismometers arranged in the form of a right-angled triangle. The instrument spacing was approximately 0.3 km. An attempt was made to estimate direction of wave propagation and apparent velocity by measuring phase differences between

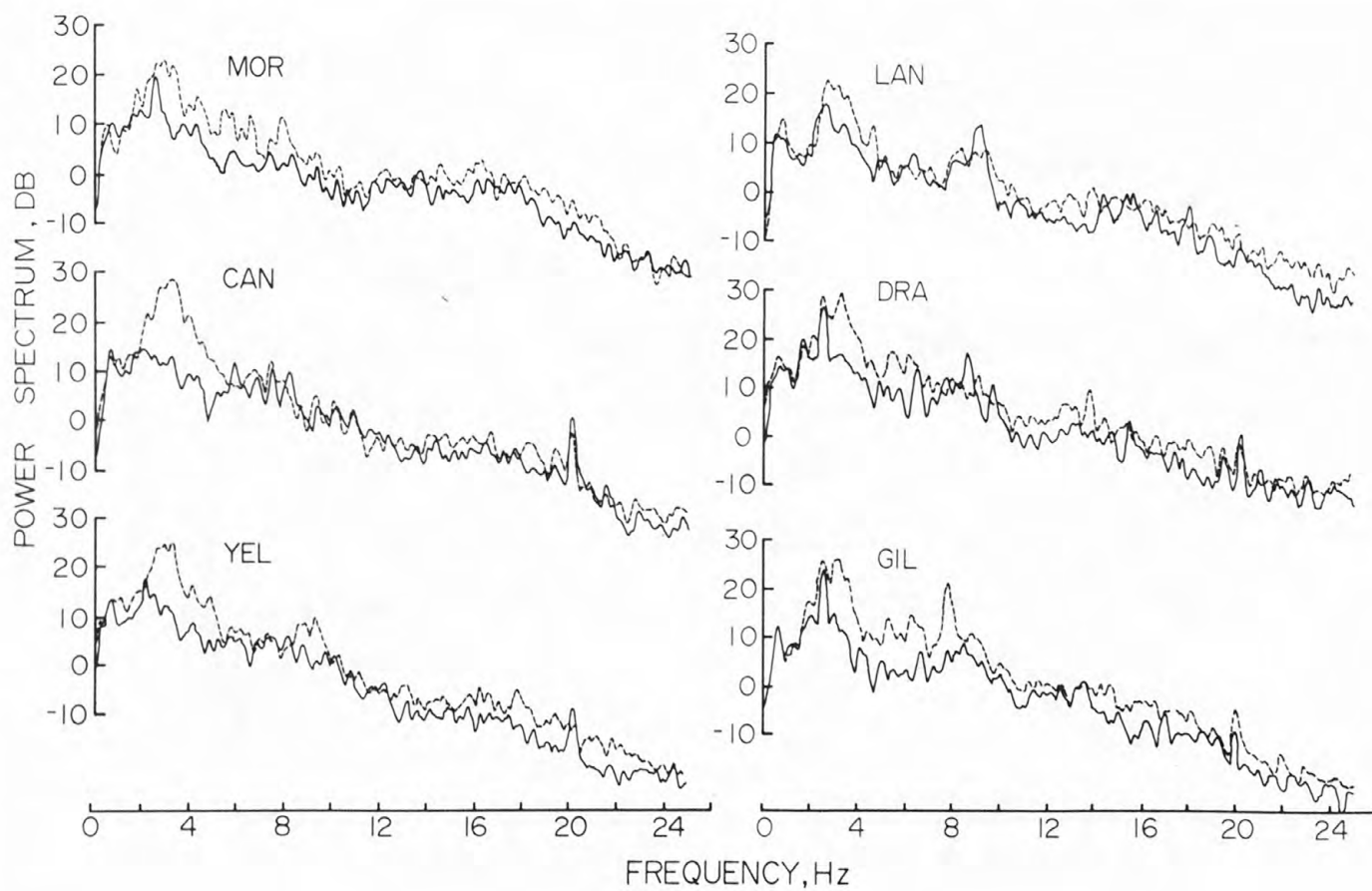


Fig. 16. Noise spectra at stations along the northern boundary of the East Mesa area. The dashed and solid lines show spectra of highest and lowest levels of noise during a four-hour recording period from midnight to 4 a.m.

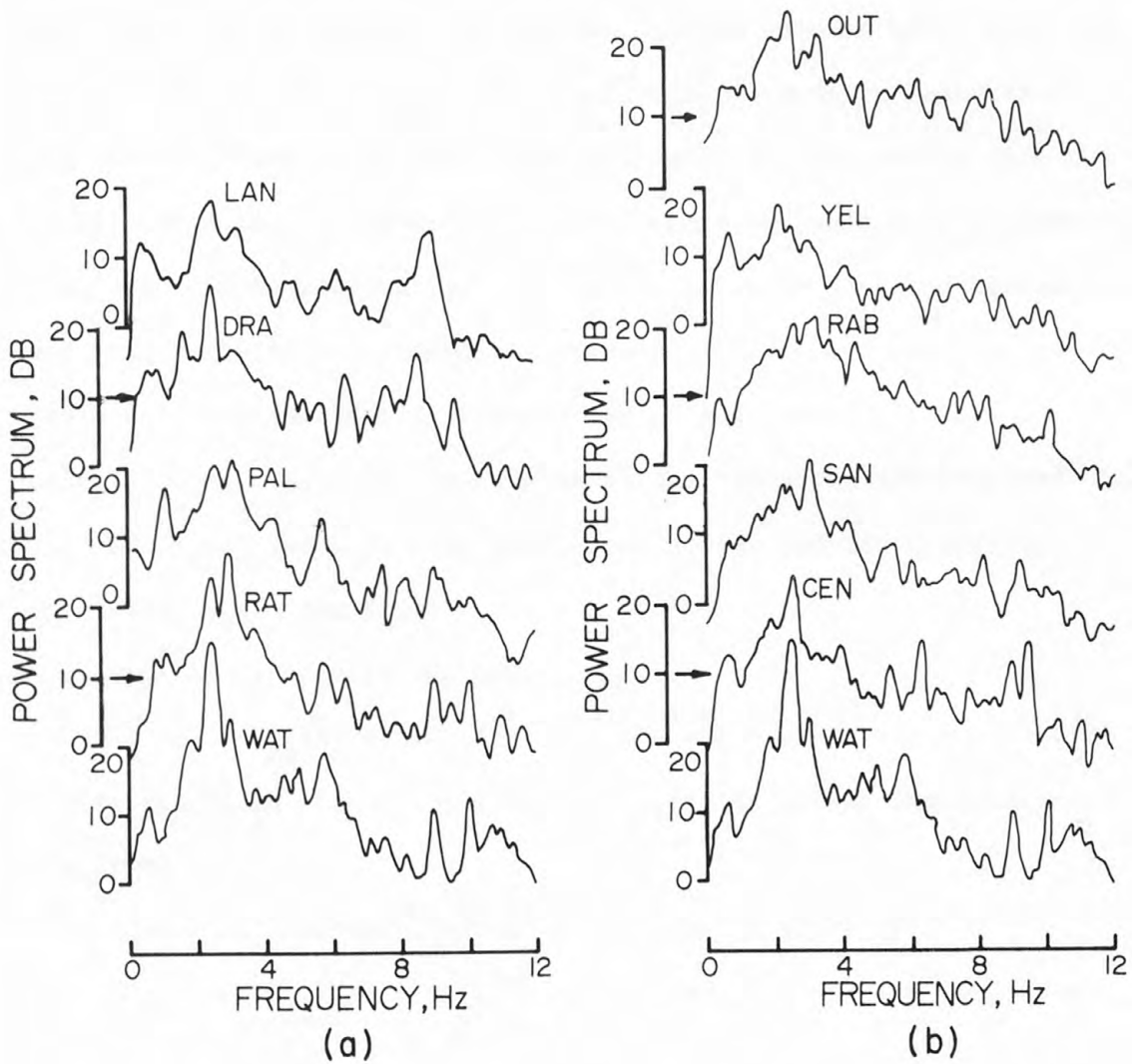


Fig. 17. Spectra of lowest levels of noise during a four-hour recording period from midnight to 4 a.m. (a) at a group of stations along an approximate northeast profile, and (b) at a group of stations along the western boundary of the East Mesa area.

waves recorded by pairs of instruments in each array. The problem would have been simple if there was visual coherence. Except at WAT and COY where the predominant noise was the 2.5 Hz waves produced by PD4, there was no obvious correlation between seismic waves recorded by the arrays. In spite of this difficulty we computed coherence¹ and phase difference between pairs of digitized time series from the arrays using the technique for single records discussed by Blackman and Tukey (1958) and modified for record pairs by Munk, Snodgrass and Tucker (1959). A Biomedical Computer Program for spectral and cross-spectral analysis of time series (Dixon, 1967) was used in the calculations. The basic principles of the technique are outlined below:

Let $X_A(t)$ and $X_B(t)$ represent time series and let their power spectra be $S_A(f)$ and $S_B(f)$.

The cross-spectra are defined as

$$S_{AB}(f) = C_{AB}(f) + i Q_{AB}(f) \text{---(1)}$$

$C_{AB}(f)$ is called the co-spectrum and $Q_{AB}(f)$ is called the quadrature-spectrum.

Square of coherence between the series is given by

$$R_{AB}^2(f) = \frac{C_{AB}^2(f) + Q_{AB}^2(f)}{S_A(f) \cdot S_B(f)} \text{---(2)}$$

Phase shift (in radians) of series $X_B(t)$ with respect to series $X_A(t)$ is

$$\phi_{AB}(f) = \arctan \frac{Q_{AB}(f)}{C_{AB}(f)} \text{---(3)}$$

¹ Note: Coherence is a measure of the degree of correlation between two time series. It is usually expressed as (coherence)². For two series of perfect sine waves (coherence)² is 1. For two time series of random numbers (coherence) is 0.

In the computer program the phase difference is normalized by dividing by 2π to convert the unit from radians to circles.

Using this method the following quantities were calculated:

$S_1(f), S_2(f), S_3(f)$ - Spectra of data from instruments

1, 2, 3.

$R_{12}^2(f)$ - (coherence)² between channels 1
and 2 at frequency f .

$R_{32}^2(f)$ - (coherence)² between channels 3 and 2 at
frequency f .

$\emptyset_{12}(f)$ - Phase shift of channel 2 with respect to
channel 1 at frequency f .

$\emptyset_{32}(f)$ - Phase shift of channel 2 with respect to 3
at frequency f .

For these computations 2048 points were used. Lag was set at 125, thus giving a frequency resolution of 0.2 Hz. Computations were carried out only for the quietest noise sample at each station.

Spatial variation of coherence. S, R^2 and \emptyset were computed for 11 stations, WAT, COY, SAN, RAB, OUT, RAT, SID, PRA, LIZ, DRA, and MOR. Typical variation of $R_{12}^2(f)$ and $R_{32}^2(f)$ in the frequency band 0-5 Hz together with $S_1(f)$ are shown in Figures 18a-18c. (Values of $R^2 > 0.1$ are considered significant).

Peaks in R^2 can be seen around 2.5 Hz at every station from the noise generated by PD4. Coherence at this frequency can be detected throughout the region. At COY which is 4.5 km from PD4, $R_{12}^2(f)$ and $R_{32}^2(f)$ are nearly 0.9 corresponding to the spectral peak. (Figure 18a). Station DRA is an example of the existence of a coherence peak without a spectral peak (Figure 18c).

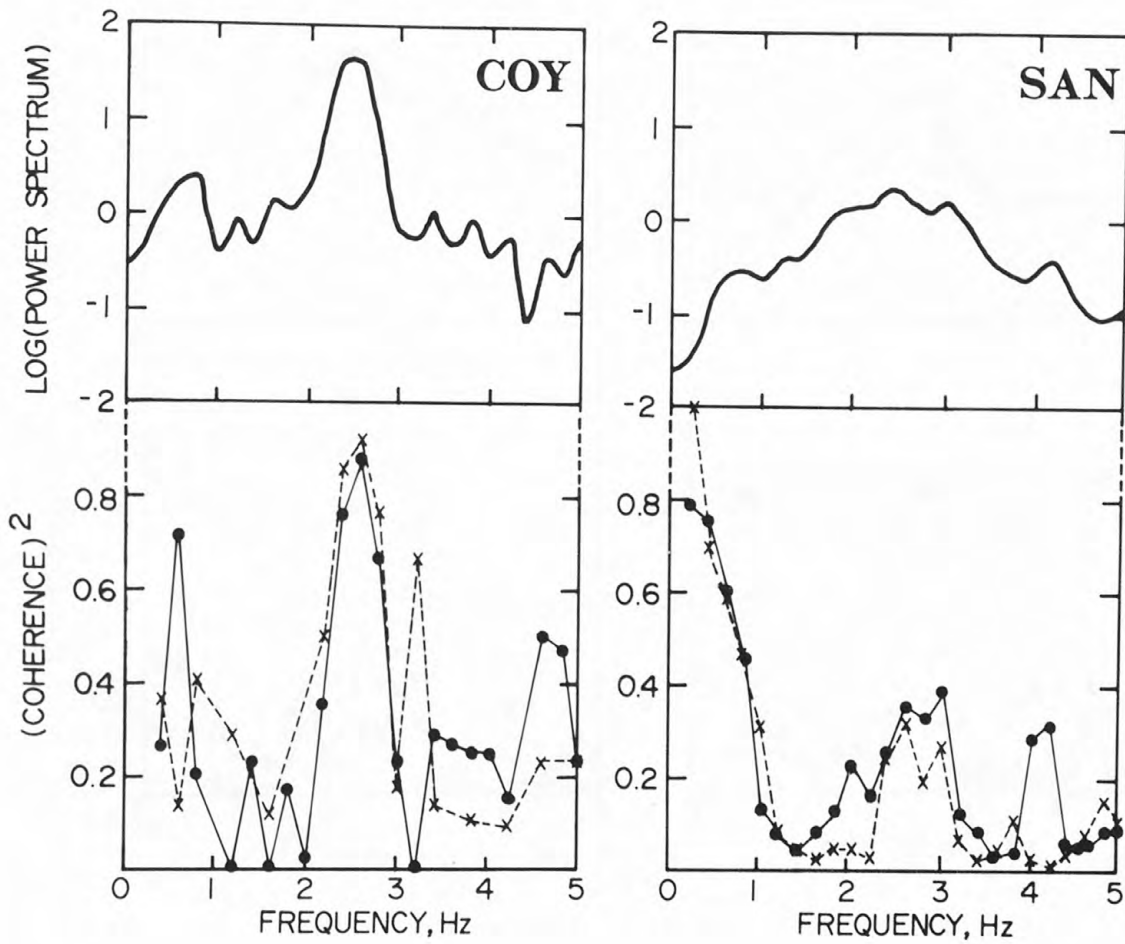


Fig. 18a. Spectra of one channel each of three element L-shaped arrays COY and SAN are shown at the top. $(\text{Coherence})^2$ between the central instrument and the first instrument is shown by solid line. $(\text{Coherence})^2$ between the central instrument and the third instrument is shown by dashed line.

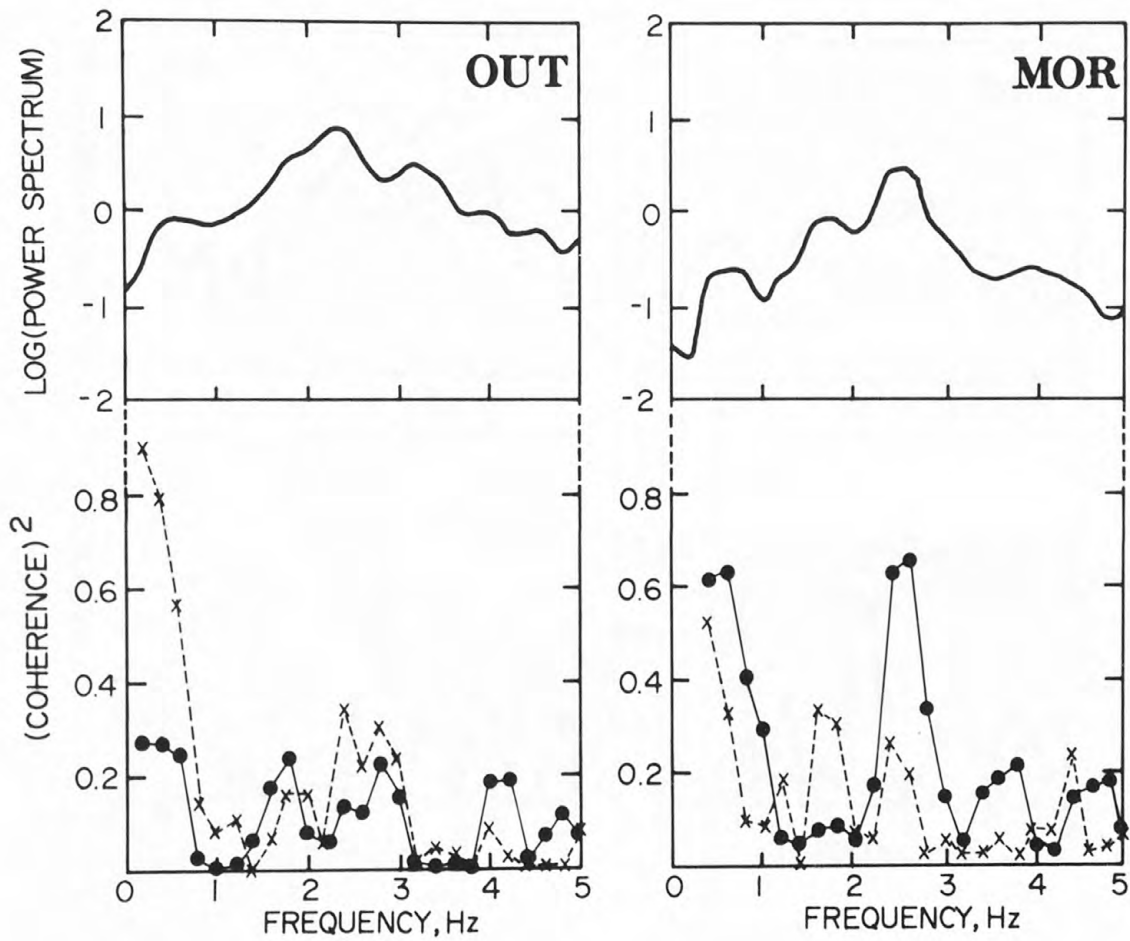


Fig. 18b. Spectra of one channel each of three-element L-shaped arrays OUT and MOR are shown at the top. $(\text{Coherence})^2$ between the central instrument and the first instrument is shown by solid line. $(\text{Coherence})^2$ between the central instrument and the third instrument is shown by dashed line.

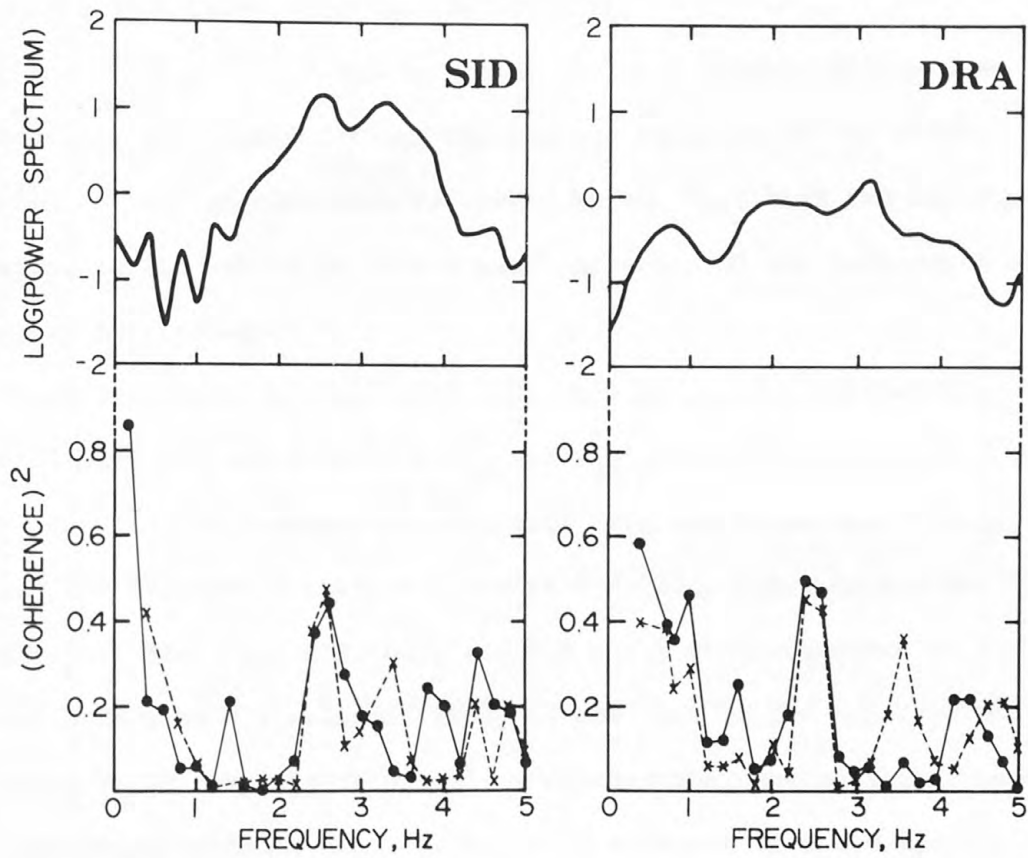


Fig. 18c. Spectra of one channel each of three-element L-shaped arrays SID and DRA are shown at the top. $(\text{Coherence})^2$ between the central instrument and the first instrument is shown by solid line. $(\text{Coherence})^2$ between the central instrument and the third instrument is shown by dashed line.

High coherence is consistently seen below 1 Hz at all stations. In most cases spectral peaks with values 1-2 orders of magnitude less than the main peaks occur in the frequency band 0.4-0.8 Hz. We think that these low-frequency peaks are from oceanic microseisms (Haubrich, 1967) seen through the low-cut response of our seismic system. The high coherence is caused by the fact that the instrument spacing in the arrays is only a small fraction of the wavelength of oceanic microseisms.

To bring out the degree of coherence at various frequencies the number of times when both R_{12}^2 and R_{32}^2 exceeded 0.1 were plotted as a function of frequency, using data from the 11 arrays. (Figure 19). The distribution shows peaks at 0.4, 2.4, 3.2, and 4.4 Hz. Since RAT, SID, PRA, LIZ, DRA, and MOR which show coherence at 3.2 and 4.4 Hz form a consistent group to the east of the MESA thermal anomaly it is tempting to speculate whether the coherence is caused by geothermal seismic noise propagating outwards from the anomaly. The lack of coherence at these frequencies at SAN, and RAB which are closer to the anomaly is not a serious objection to this hypothesis because proximity to source destroys coherence. (A point source gives much higher coherence than an extended source at an array. Hence the array has to be sufficiently far to "see" the source as a point for good coherence). The real difficulty is that we are not able to determine whether these peaks of coherence are sidebands (generated by cross-spectral analysis) or higher modes (caused by propagation in layered media) of the 2.5 Hz peak. Studies of direction of travel of 3.4 and 4.4 Hz waves should point to their source, but unfortunately our array spacing was too large and no definite

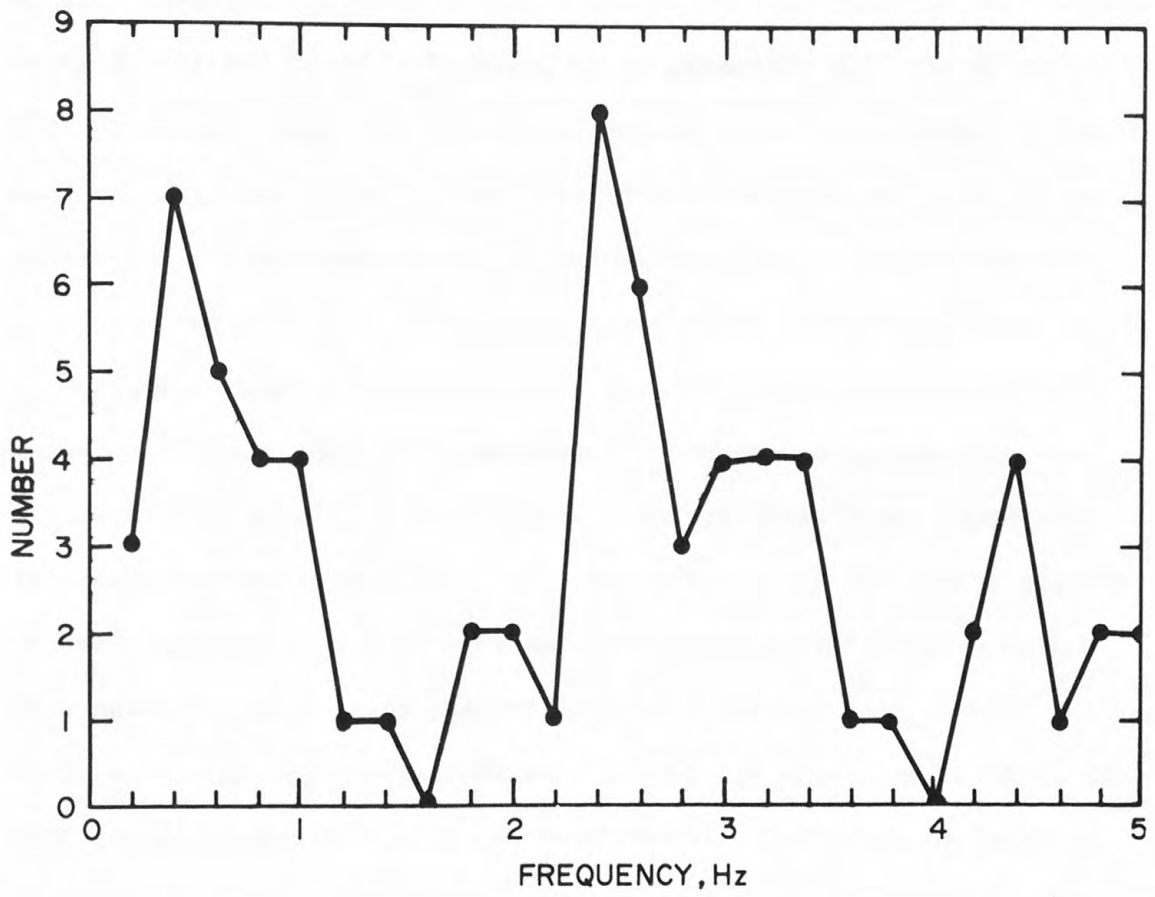


Fig. 19. Distribution of the number of times $(\text{Coherence})^2$ exceeded 0.1 for various frequency bands.

conclusions could be reached on the nature of this noise. This problem is discussed in the next section.

Direction studies. Apparent velocity and direction of travel of seismic waves at different frequencies can be calculated at each array using $\phi_{12}(f)$ and $\phi_{32}(f)$. However, it is necessary that the array spacing be much less than one wavelength as otherwise a phase difference of $(\phi \pm 2\pi n)$ where n is an integer will be measured as ϕ in the cross-spectral analysis program. Unfortunately it appears that the array spacing used (0.3 km) was too large, thus making the phase values non-unique. This can be illustrated by using results from station WAT, where it is known that the predominant 2.5 Hz waves arrive from PD4.

A typical plot of seismic noise from the three array components (Figure 20) shows highly coherent waves. The phase difference between channels using the plot as well as the cross-spectral program both show that channel 2 leads channel 1 by 0.15 sec and lags channel 3 by 0.06 sec, giving an apparent velocity of 1.8 km/sec and azimuth of 223° (measured counter-clockwise from north). The actual azimuth to PD4 is 135° . Nine possible solutions can be obtained by adding $\pm 2\pi$ to the phase components. These velocities and azimuths are schematically shown in Figure 21. The correct azimuth is given for phase combination $(\phi_{21}(f) - 2\pi)$ and $(\phi_{23}(f) - 2\pi)$. The phase velocity for this combination is 0.5 km/sec, which is more reasonable than 1.8 km/sec for surface waves propagating in a sedimentary layer with low compressional wave velocity. Using this technique it was possible to get solutions for azimuth which point to PD4 with apparent velocities in the range of 0.4-0.7 km/sec. A search was made to look for solutions pointing to

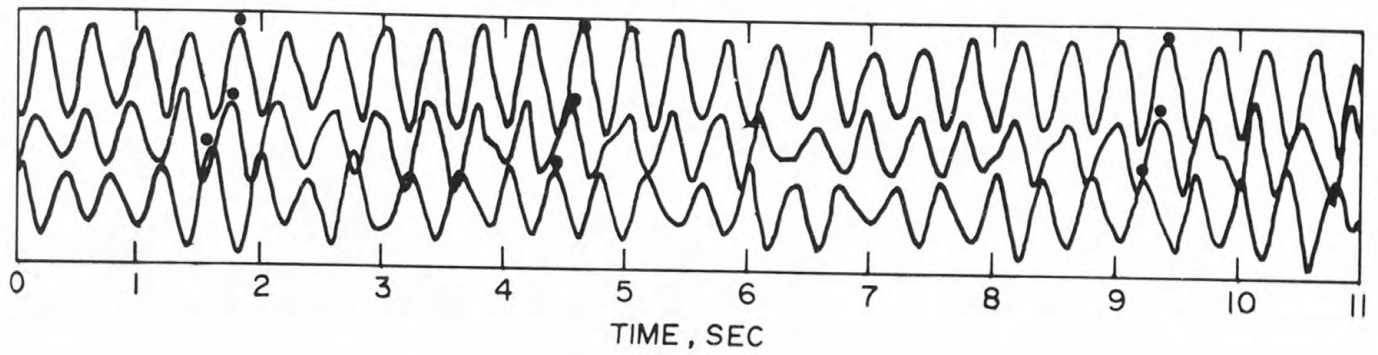


Fig. 20. Sample of three-element array seismograms at WAT. The dots indicate coherent phases.

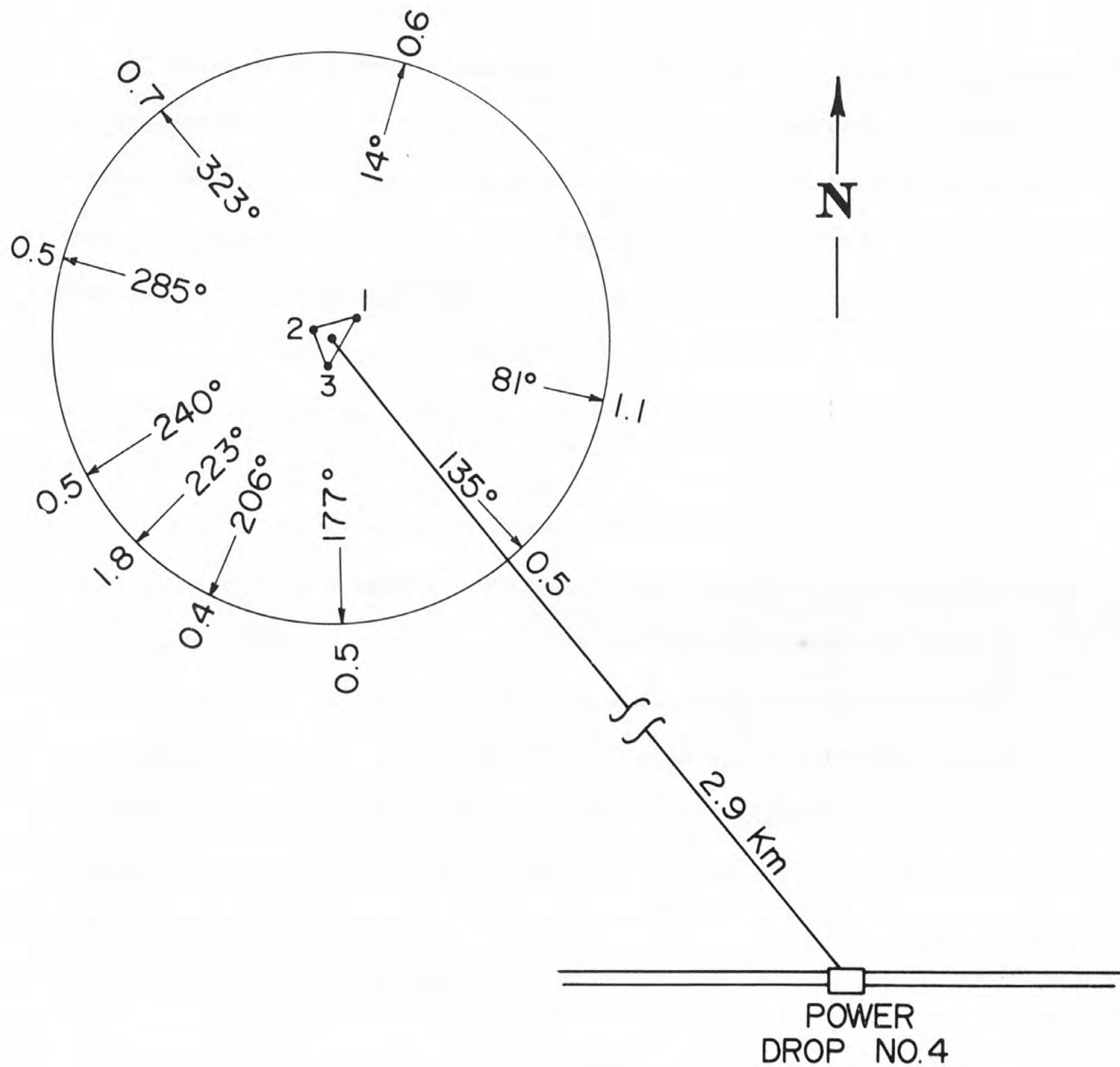


Fig. 21. Results of direction studies of 2.5 Hz noise using the three-element array WAT. The triangle with numbers shows the array. The arrows indicate azimuth of noise source as seen by the array. The number before the arrow is the azimuth in degrees and the number after the arrow is the velocity of wave in km/sec.

the Mesa thermal anomaly using phase measurements at 3.5 and 4.4 Hz. In all cases one or more plausible solutions could be found. In view of the uncertainties involved in the selection of appropriate phase values we are unable to say whether or not we have detected geothermal noise propagating outwards from the Mesa anomaly. It was virtually impossible to detect any coherence by visual examination of array records at any stations except WAT and COY. Seismic arrays with 50m instrument spacing are required for direction studies in the East Mesa area.

Our array spacing was too small for finding apparent velocities and azimuths of the highly coherent 0.4-0.8 Hz waves. Though the phase uncertainty was not present, the inaccuracies in measuring the small phase difference values resulted in a wide range of velocities and azimuths. About 40% of the values indicated waves arriving from the west with a velocity of 1.5-2.5 km/sec. This supports our earlier conjecture that the low-frequency noise is part of regional oceanic microseisms.

CONCLUSIONS

The main conclusion is that we were unable to detect seismic noise over the Mesa thermal anomaly that could not be attributed to cultural noise. Noise from freeway traffic, canal, agricultural activity and a power drop was quite strong over the anomaly, and the amplitude of geothermally generated noise, if present, is less than that of cultural noise. Arrays with 50 m or less spacing may give some definite conclusions regarding the presence or absence of a noise anomaly in this area. Seismic noise surveys using such arrays over other thermal anomalies in Imperial Valley are needed to answer the interesting

question of whether seismic noise is generated by hydrothermal systems of the type found in that region.

ACKNOWLEDGEMENTS

John Coakley, John Roller, Wayne Jackson, James Gibbs, and Steven Gallanthine did the field work. Jeanne Taylor played back the tapes and digitized the data. Tim Hitchcock assisted in preparing the diagrams. Patrick Muffler critically read the manuscript and made a number of helpful comments and suggestions.

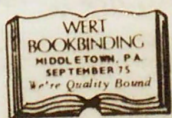
REFERENCES

- Blackman, R. B., and J. W. Tukey, The Measurement of Power Spectra, Dover Publications, New York, 1958.
- Clacy, G. R. J., Geothermal Ground Noise Amplitude and Frequency Spectra in the New Zealand Volcanic Region, J. Geophys. Res., 73, 5377-5384, 1968.
- Dixon, W. J. (Editor), Biomedical Computer Programs, University of California Press, Berkeley and Los Angeles, 459-482, 1967.
- Douze, E. J., and G. G. Sorrells, Geothermal Ground-noise Surveys, Geophysics, 37, 813-824, 1972.
- Eaton, J. P., M. E. O'Neill, and J. N. Murdock, Aftershocks of the 1966 Parkfield-Cholame, California, earthquake: a detailed study, Bull. Seismol. Soc. Amer., 60, 1151-1197, 1970.
- Eng, Kenneth, and R. W. Decker, Anomalous Microseisms in Surprise Valley, California (Abs), Proceedings of the U. S. - Japan Co-op Science Seminar on Utilization of Volcanic Energy (In Press), 1974.
- Geothermal Staff of Teledyne-Geotech, Geothermal Noise Survey of the East Mesa Area, Imperial Valley, California, Teledyne-Geotech Technical Report No. 72-19, 17p, 1972.
- Goforth, T. T., E. J. Douze, and G. A. Sorrells, Seismic Noise Measurements in a Geothermal Area, Geophys. Prospecting, 20, 76-82, 1972.
- Haubrich, R. A., Microseisms, International Dictionary of Geophysics, Pergamon Press, New York, 2, 975-977, 1967.
- Iyer, H. M., and Tim Hitchcock, A Seismic Noise Survey in Long Valley, California (Abs), EOS (Trans. Am. Geophys. Union), 54, 1212, 1973.
- Iyer, H. M., and Tim Hitchcock, Seismic Noise Measurements in Yellowstone National Park, Geophysics (In Press), 1974.
- Munk, W. H., F. E. Snodgrass, and M. J. Tucker, Spectra of Low-frequency Ocean Waves, Bull. Scripps Inst. Oceanog., 7, 283-362, 1959.
- Swanberg, Chandler A., Preliminary Results of Geothermal Well Mesa 6-2, Mesa Anomaly, Imperial Valley, California (Abs), EOS (Trans. Am. Geophys. Union), 54, 1215, 1973.

U. S. Bureau of Reclamation, Geothermal Resource Investigations,
Imperial Valley, California, Test Well Mesa 6-1, Special Report,
February 1973.

Welch, P. D., The Use of the Fast Fourier Transform for the Estimation
of Power Spectra, IEEE Trans. on Audio and Electroacoustics,
AU-17, 151-157, 1969.

Whiteford, P. C., Ground Movement in the Waiotapu Geothermal Region,
New Zealand, Geothermics (Special Issue on Proceedings of the
United Nations Symposium on the Development and Utilization
of Geothermal Resources, 2 (Pt. II), 478-486, 1970.



USCS LIBRARY-RESTON



3 1818 00076919 8